EGG-CAAP-5191

June 1980

TRAC-P1A CALCULATIONS FOR A 200% HOT LEG BREAK AND A 200% HOT LEG BREAK SIMULTANEOUS WITH A RUPTURE OF 16 STEAM GENERATOR TUBES IN A PRESSURIZED WATER REACTOR

M. A. Bolander

U.S. Department of Energy
Idaho Operations Office • Idaho National Engineering Laboratory

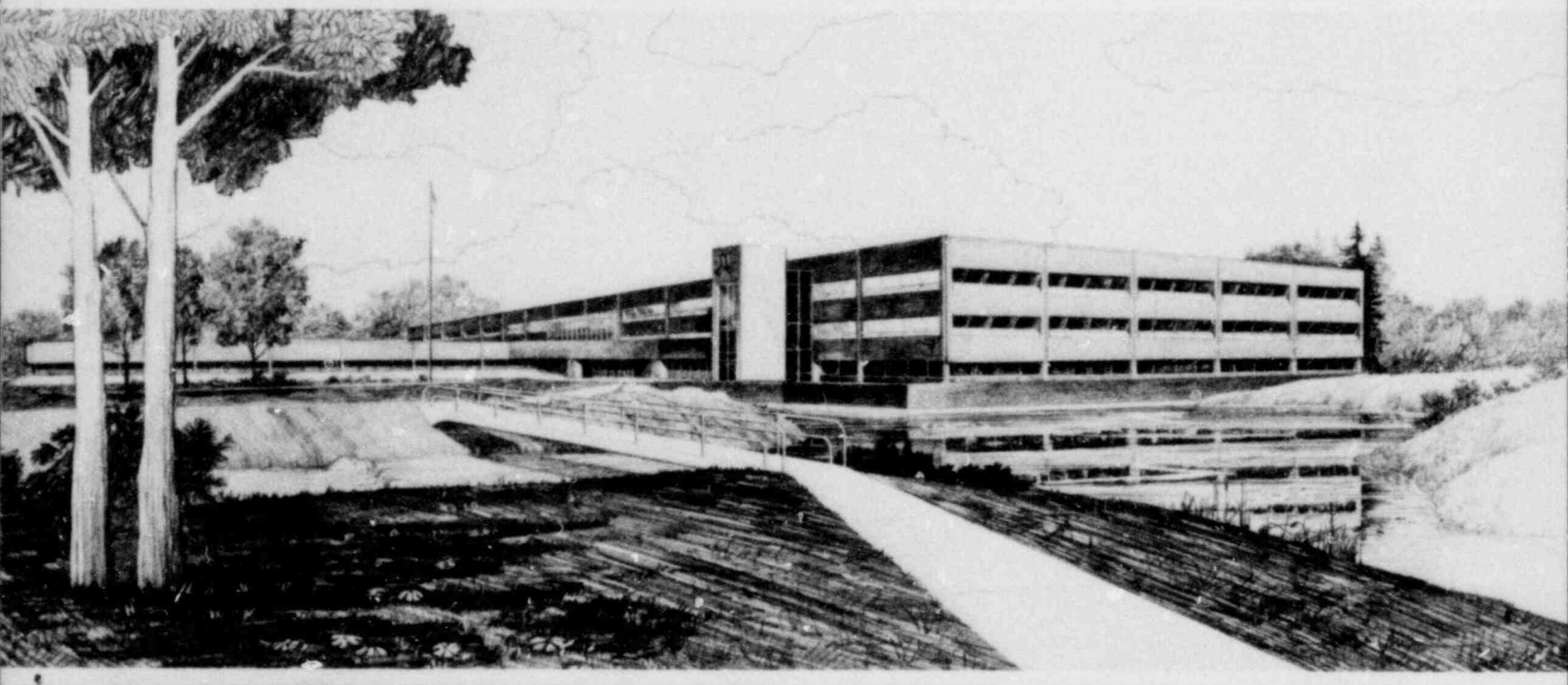

Prepared for the
U.S. Nuclear Regulatory Commission
Under DOE Contract No. DE-AC07-76ID01570
NRC FIN No. A6047

EG&G Idaho

EG&G Idaho, Inc.

FORM EG&G-398
(Rev. 11-79)

INTERIM REPORT

Accession No. _____

Report No. EGG-CAAP-5191

Contract Program or Project Title: Code Assessment and Applications Program

Subject of this Document: TRAC-P1A Calculations for a 200% Hot Leg Break and a 200% Hot Leg Break Simultaneous with a Rupture of 16 Steam Generator Tubes in a Pressurized Water Reactor

Type of Document: Preliminary Assessment Report

Author(s): M. A. Bolander

Date of Document: June 1980

Responsible NRC Individual and NRC Office or Division: F. Odar, NRC-RSR

This document was prepared primarily for preliminary or internal use. It has not received full review and approval. Since there may be substantive changes, this document should not be considered final.

EG&G Idaho, Inc.
Idaho Falls, Idaho **83415**

Prepared for the
U.S. Nuclear Regulatory Commission
Washington, D.C.
Under DOE Contract No. **DE-AC07-76ID01570**
NRC FIN No. A6047

INTERIM REPORT

ABSTRACT

The TRAC-P1A computer code developed by Los Alamos Scientific Laboratory was used to perform two calculations for a large Pressurized Water Reactor (PWR): A 200% hot leg break and a 200% hot leg break simultaneous with a rupture of 16 steam generator tubes. The plant modeled for the calculations was the Westinghouse Zion I PWR. The calculated results for a 200% hot leg break and the effects of the rupture of 16 steam generator tubes simultaneous with a 200% hot leg break are discussed.

ACKNOWLEDGEMENTS

The author of this report wishes to thank the contributors, supporters and reviewers. J. R. Larson and P. D. Wheatley contributed significantly to the development and analysis of the calculations. A. C. Peterson and C. D. Fletcher provided important advice in preparation of this report.

I wish to express my appreciation to Colleen Polk, Julie Sellars and Dawnie Terry for their timely contributions to this report.

Finally, I express my appreciation to Joan Mosher in Text Processing. Her efficiency and patience have contributed much to the preparation of this report.

CONTENTS

FIGURES

TABLES

SUMMARY

The TRAC-P1A computer code, developed by Los Alamos Scientific Laboratory, was used to perform two calculations for a large PWR: a 200% hot leg break and a 200% hot leg break with 16 ruptured steam generator tubes. These calculations are part of the overall assessment program for TRAC-P1A being conducted at INEL. The Westinghouse Zion I PWR was used as the basis for the model.

The BE/EM study,[1] a PWR model developed by LASL[2] and the Safety Analysis Report[3] for the Zion I reactor were used to develop the TRAC model. A steady state run was made to obtain conditions for the transient calculations.

The two calculations had similar overall results, however some steam binding in the upper plenum prolonged core reflood in the steam generator tube rupture calculation. The cladding temperatures did not exceed 646.0 K during the calculations. The rods had completely quenched by 22.0 s in the 200% hot leg break calculation and by 23.2 s in the steam generator tube rupture calculation.

1. INTRODUCTION

The TRAC-P1A* computer code, developed at LASL (Los Alamos Scientific Laboratory), was used to perform LOCA (Loss-of-Coolant Accident) calculations at the INEL for a large pressurized water reactor. These calculations are part of the overall assessment program for TRAC-P1A being conducted at INEL. The calculations encompass hot and cold leg break locations, large to small sizes, with steam generator tube rupture as an additional parameter. The calculations cover the blowdown, refill and reflood phases of the accident.

This document reports two of the LOCA calculations: (1) a 200% hot leg break and (2) a 200% hot leg break simultaneous with the rupture of 16 steam generator tubes in one loop. The number of ruptured tubes in the 200% hot leg break calculation with a ruptured steam generator was chosen to be consistent with the corresponding cold leg break calculation reported in Reference 1. Additional TRAC PWR calculations describing large, intermediate and small cold leg breaks are reported in Reference 2.

The Westinghouse Zion I pressurized water reactor was used as the model plant for the calculations. Section 2 describes the modeling, noding and initial and boundary conditions used for the calculations. Section 3 describes the results and a discussion of the calculation and Section 4 contains the conclusions which were obtained from each of the calculations.

---

* Identified internally as TRACN1 and stored at INEL under Configuration Control Number H003885B.

2. MODEL DESCRIPTION

The calculational model was developed using the Zion I pressurized water reactor as a basis for providing input to the TRAC computer code. The input data came from three sources, the BE/EM study,[3] a PWR model developed by LASL[4] and the Safety Analysis Report for the Zion I reactor.[5] The BE/EM study was the primary source unless more complete information was available from other sources. The following sections describe the code version used, model nodalization, code options, and the initial and boundary conditions for the calculation. A detailed listing of the code input, nodalization and boundary conditions of the components can be found in Appendices A, B, and C, respectively.

2.1 Code Description

The code version used was TRAC-P1A[2] with the updates described in TRAC Newsletter No. 1.[6] The configuration control number for the input decks of the steady state and the transient models is H0078858.* 5.3 and 4.9 CPU hours were required on the CDC 176 computer at INEL to complete the 200% hot leg break and 200% hot leg break with ruptured steam generator tube calculations, respectively.

2.2 Nodalization

The TRAC-P1A model for a 200% hot leg break and a 200% hot leg break with ruptured steam generator tubes consisted of four separate loops (one broken and three intact) and a vessel as shown in Figure 1. The steady state model consisted of 548 cells representing 55 components. The transient models included the addition of the breaks and a valve component to simulate the ruptured steam generator tubes as shown in Figure 2. The

---

* The steady state model is found in Partition 1, the hot leg break is found in Partition 2 and the hot leg break with a steam generator tube rupture is found in Partition 3.

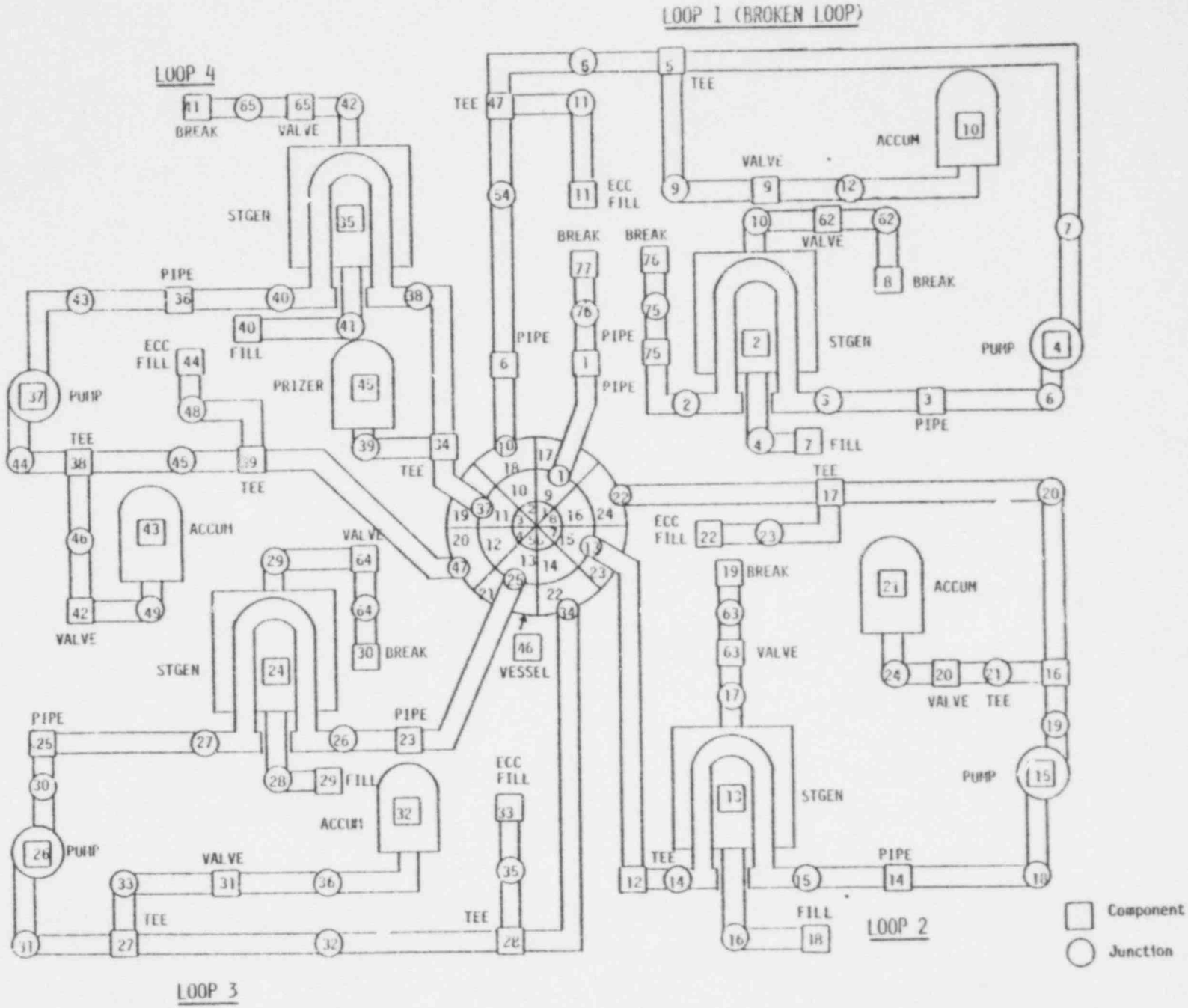

Figure 1. 200% hot leg break nodalization.

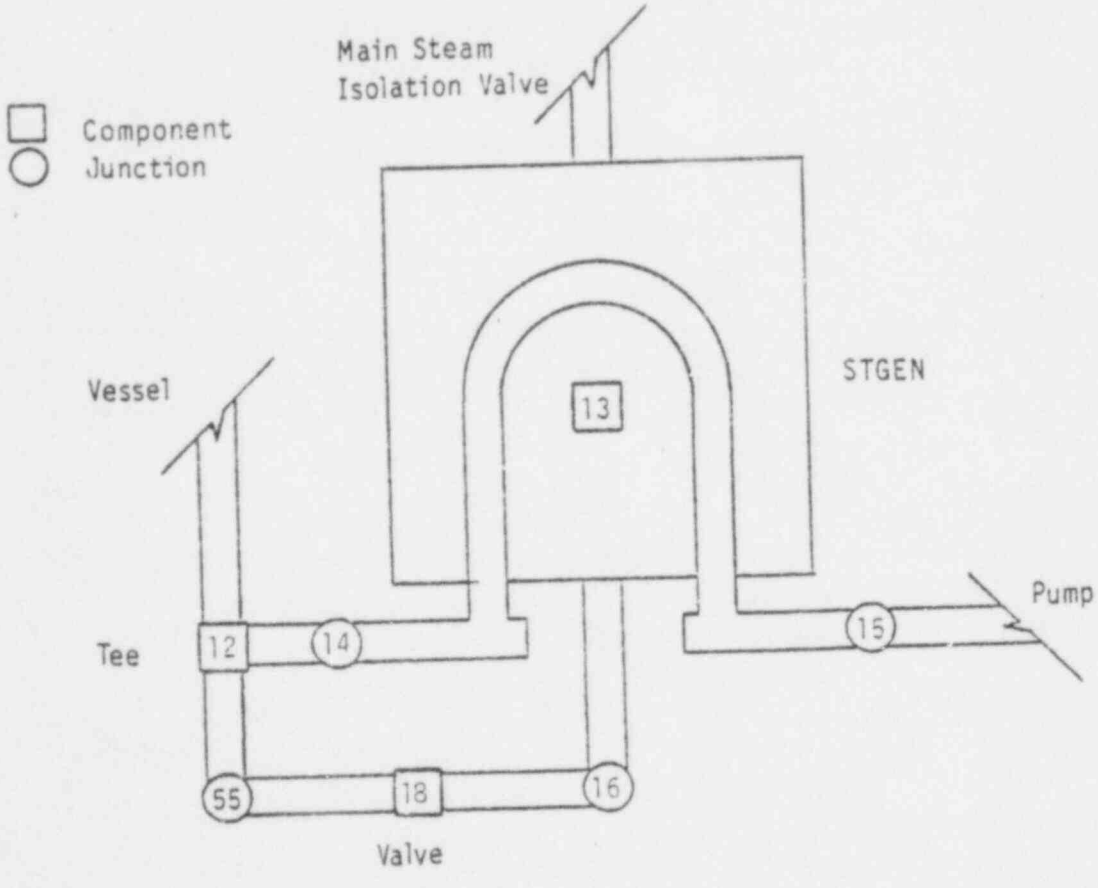

Figure 2. Steam generator tube rupture model for the 200% hot leg break simultaneous with a rupture of sixteen steam generator tubes.

number of cells for the transient models was 547 representing 57 components. For comparison the USPWR1 model developed by LASL consisted of 634 cells representing 42 components.

2.3 Code Options

Few code options exist in TRAC-P1A. A major choice concerns the friction factor correlation to be used in components other than the vessel. Based on the TRAC Developmental Assessment Report,[7] the annular flow correlation (NFF=4) was selected for all components except VALVE 18. The homogeneous flow correlation (NFF=1) was used in VALVE 18 because the sizing of the nozzle to simulate the tube rupture flow area was performed using the homogeneous flow correlation.

The option permitting the code to calculate the fuel rod gap conductance was also selected (NFCI=1). This resulted in a lower than reasonable gap conductance and a peak centerline temperature at steady state that was excessively high. The effect of this parameter on cladding surface temperature was discussed in Reference 2.

The partially implicit numerical hydrodynamics option (IHYDRO=0) was used throughout the loop piping except for the piping adjacent to the breaks where the fully implicit option (IHYDRO=1) was used. The fully implicit option was also used on the secondary side of the tees connecting the pressurizer and accumulators to the loop.

The option for determining core power versus time (IRPOP=7) was selected. The power-time table was taken from the BE/EM study.

2.4 Initial and Boundary Conditions

Initial conditions were obtained for the transient calculations by performing a steady state calculation. The system operating conditions at steady state are shown in Table 1. Appendix C describes the initial and boundary conditions applied to the model components in more detail.

TABLE 1. SYSTEM OPERATING CONDITIONS

Core power (MWt)	3228
Loop Mass Flow Rate (kg/s)	
Loop 1	4615
Loop 2	4614
Loop 3	4613
Loop 4	4601
Hot Leg Entrance Temperature (K)	
Loop 1	583.2
Loop 2	583.0
Loop 3	583.2
Loop 4	583.2
Cold Leg Exit Temperature (K)	
Loop 1	550.5
Loop 2	550.5
Loop 3	550.6
Loop 4	550.5
Pump Head (MPa)	
Loop 1	0.606
Loop 2	0.644
Loop 3	0.644
Loop 4	0.618
Upper Head Temperature (K)	569.4
Core ΔT (K)	33.2
Core ΔP (MPa)	0.085
Average Rod Peak Power Density (kw/m)	31.73

3. RESULTS AND DISCUSSION

The results of the TRAC-P1A calculation of the 200% hot leg break and 200% hot leg break with steam generator tube rupture* are discussed below. A brief description of the major events pertinent to both calculations will be presented first followed by a detailed discussion of the individual calculations.

3.1 Major Events of Calculations

Table 2 lists the sequence of significant events in the calculations. The break occurred at time 0.0 s with a trip signal being sent to the steam generator secondary main feedwater and the steam generator secondary main steam isolation valve. At 0.532 s the reactor scrammed. By 1.5 s the steam generator main steam isolation valves were closed. Between 1.1 and 1.5 s the steam generator main feedwater flow was shut off and between 1.5 and 5.6 s the steam generator auxiliary feedwater flow was increased from 0 to 25.6 kg/s. At 3.08 s (3.04 s for the steam generator tube rupture calculation) HPIS injection began. The broken loop (loop 1) accumulator flow began at 12.4 s. The flow in loops 2, 3 and 4 accumulators began at 12.56, 12.6 and 12.6 s respectively. For the steam generator tube rupture calculation, the broken loop (loop 1) accumulator flow was initiated at 12.35 s with injection from loop 2, 3 and 4 accumulators at 12.66, 12.71 and 12.72 s respectively. The start of refill for the hot leg break calculation was at 15.6 s, 15.8 s for the steam generator tube rupture calculation. Two phase core reflood had begun by 18.6 s in both calculations. The rod temperatures at the top of the core had turned around at 20.4 s in the hot leg break calculation and at 21.8 s in the steam generator tube rupture calculation. By 21.4 s the lower

---

* Throughout the remainder of this report the 200% hot leg break calculation and the 200% hot leg break simultaneous with the rupture of 16 steam generator tubes calculation will be referred to as the hot leg break calculation and the steam generator tube rupture calculation, respectively.

TABLE 2. MAJOR EVENTS OF THE HOT LEG BREAK CALCULATIONS

	Time of Event (s)	
	200% Hot Leg Break	200% Hot Leg Break With Steam Generator Tube Rupture
Break	0.0	0.0
Reactor Scram	0.532	0.532
Loop 1 Accumulator on	12.40	12.355
Loop 2 Accumulator on	12.56	12.66
Loop 3 Accumulator on	12.60	12.707
Loop 4 Accumulator on	12.60	12.723
ECC Injection (HPIS, LPIS, Charging) on	3.08	3.04
Steam Generator Secondary Main Feedwater off	1.1-1.5	1.1-1.5
Steam Generator Secondary Auxiliary Feedwater on	1.5-5.6	1.5-5.6
Steam Generator Secondary Main Steam Isolation Valve Closed	0-1.5	0-1.5
Pressurizer Empty	21.2	21.2
Start of Refill	15.6	15.8
Start of Reflood	18.6	18.6
Lower Plenum Liquid Full	21.4	21.4
Maximum Average Clad Temperature (K)	644.0	646.0
Core Rods Quenched	22.0	23.2

plenum was completely liquid full and liquid was flooding the core. The core had completely filled by 25.0 s in the hot leg break calculation and 23.6 s in the steam generator tube rupture calculation.
The hot leg break calculation was terminated at 29.16 s and the steam generator tube rupture calculation was terminated at 25 s because the fuel rods had quenched and the core was liquid full.

3.2 200% Hot Leg Break Calculation

This section describes the response of the 200% hot leg break calculation. The broken loop (loop 1) response will be discussed first then an intact loop (loop 2 and loop 3) response, followed by the pressurizer loop (loop 4) response. The vessel thermal-hydraulic behavior will then be discussed.

At the initiation of the break the system experienced a rapid subcooled depressurization to 10 MPa as shown in Figure 3. Mass flow out the breaks of loop 1 was rapid (between 10,000 and 22,000 kg/s) as seen in Figures 4 and 5. The flow in the loop side (loop 1) of the break reversed. The fluid began to flash (beginning in the upper plenum and proceeding to the hot legs) due to a liquid superheat. Vapor generation from flashing caused the depressurization rate to decrease between 0.1 and 0.6 s. At 0.6 s the volume addition from vapor generation exceeded the volumetric flow out the break and the system repressurized to 9.1 MPa. The pressure remained constant for about 0.6 s because of an equalization in vapor generation and volumetric flow rate out the break. At 1.6 s the volumetric increase in the primary due to vapor generation dropped below the volumetric flow rate out the break and system depressurization continued. The repressurization response was delayed in the loop side of the break as seen in Figure 5 because the pressure response had to travel through the vessel and around the broken loop to the break.

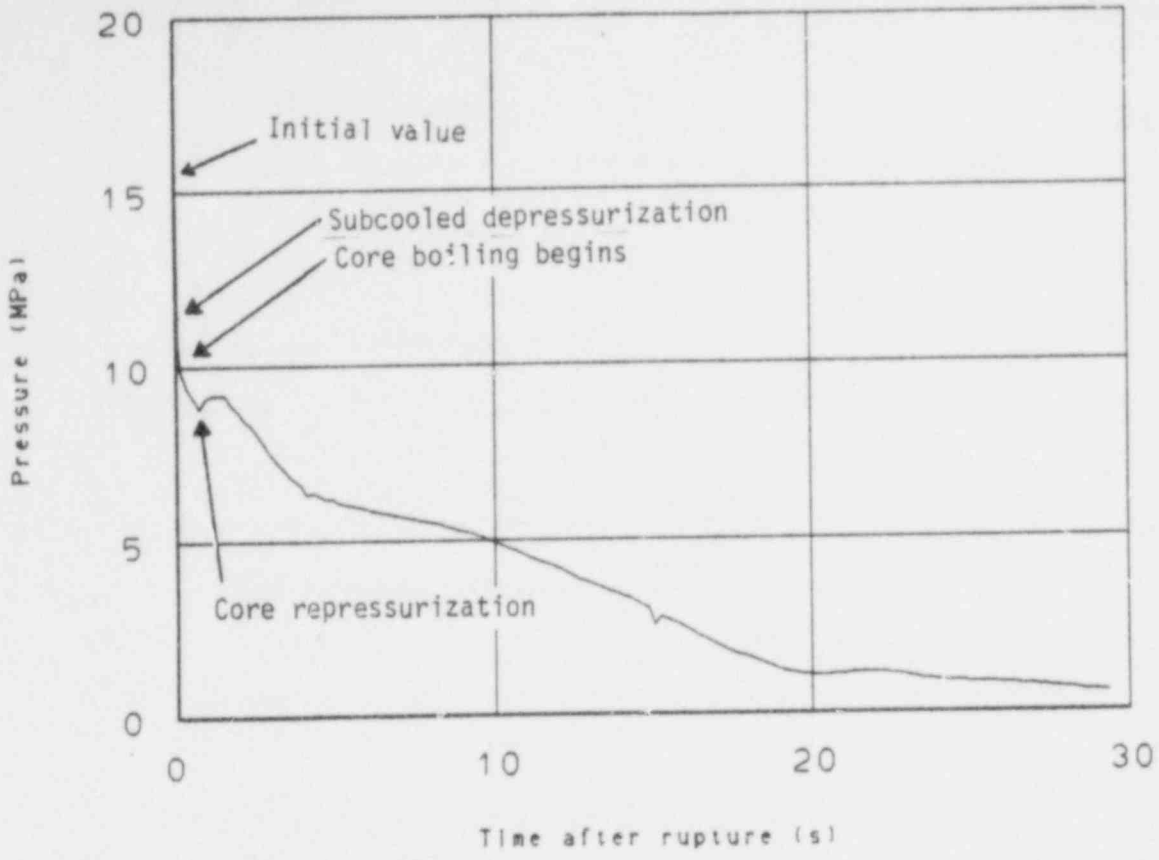

Figure 3. Broken loop (Loop 1) hot leg pressure, near the vessel.

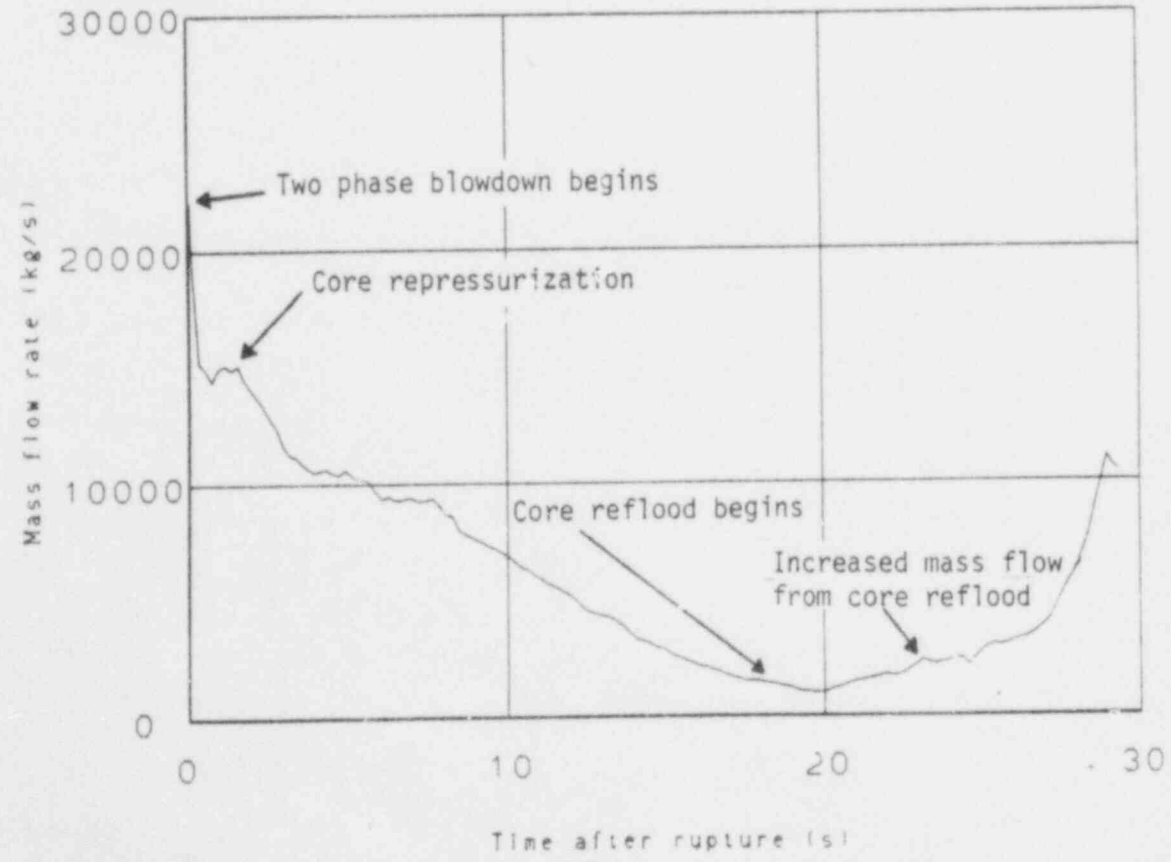

Figure 4. Break mass flow rate (Loop 1), vessel side of break.

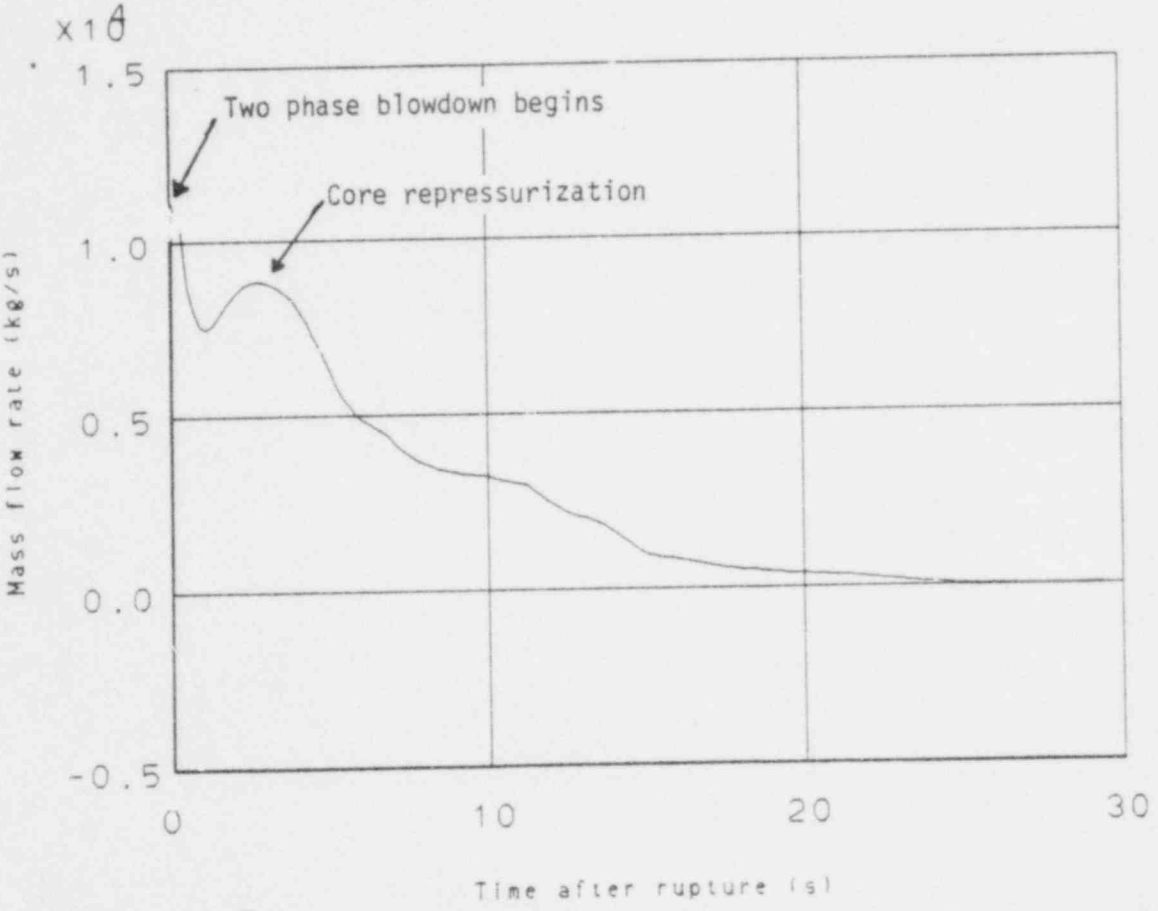

Figure 5. Break mass flow rate (Loop 1), loop side of break.

At 3 s the broken loop (loop 1) HPIS/LPIS injection began. Localized condensation effects from the subcooled HPIS/LPIS injection had minimal effects on the broken loop behavior. At 12.4 s the system pressure dropped below the accumulator valve setpoint in the broken loop and the accumulator began injecting subcooled liquid into the broken loop (loop 1). At the time of accumulator flow initiation, the loop void fraction was about 0.90. With the injection of the accumulator fluid the broken loop began to fill up with liquid as shown by the decrease in the void fraction in the broken loop in Figure 6.* The loop was completely liquid filled by about 17 s.

At 15.6 s the flow in the broken loop cold leg reversed and began to inject liquid into the inlet annulus as shown in Figure 7. The negative loop pressure differential created by the break had decreased enough to approach the positive pressure differential created by the rotating pump. Also the pressure in the downcomer had dropped slightly below the broken loop cold leg pressure because of condensation from subcooled liquid injected into the downcomer from the intact loops. These effects caused the flow to reverse in the broken loop cold leg.

Mass flow in the pump suction leg of the broken loop became stagnant after the flow reversed in the cold leg as seen in Figure 8. The steam generator evaporated the liquid that remained in the primary tubes after the flow reversal in the cold leg. The evaporated liquid exited through the break.

By 17 s the cold leg was liquid full, injecting liquid into the inlet annulus, down the downcomer and filling the vessel lower plenum. At 18.6 s two phase core reflood had begun. The two phase mixture was forced up the core, cooling the rod clad temperatures in the bottom of the core. By 21.4 s the lower plenum was liquid full. The liquid progressed up the core, quenching the rods. A two phase mixture was generated as liquid

---

* The figures shown throughout the report are the response in one cell of the model but are representative of the behavior being discussed.

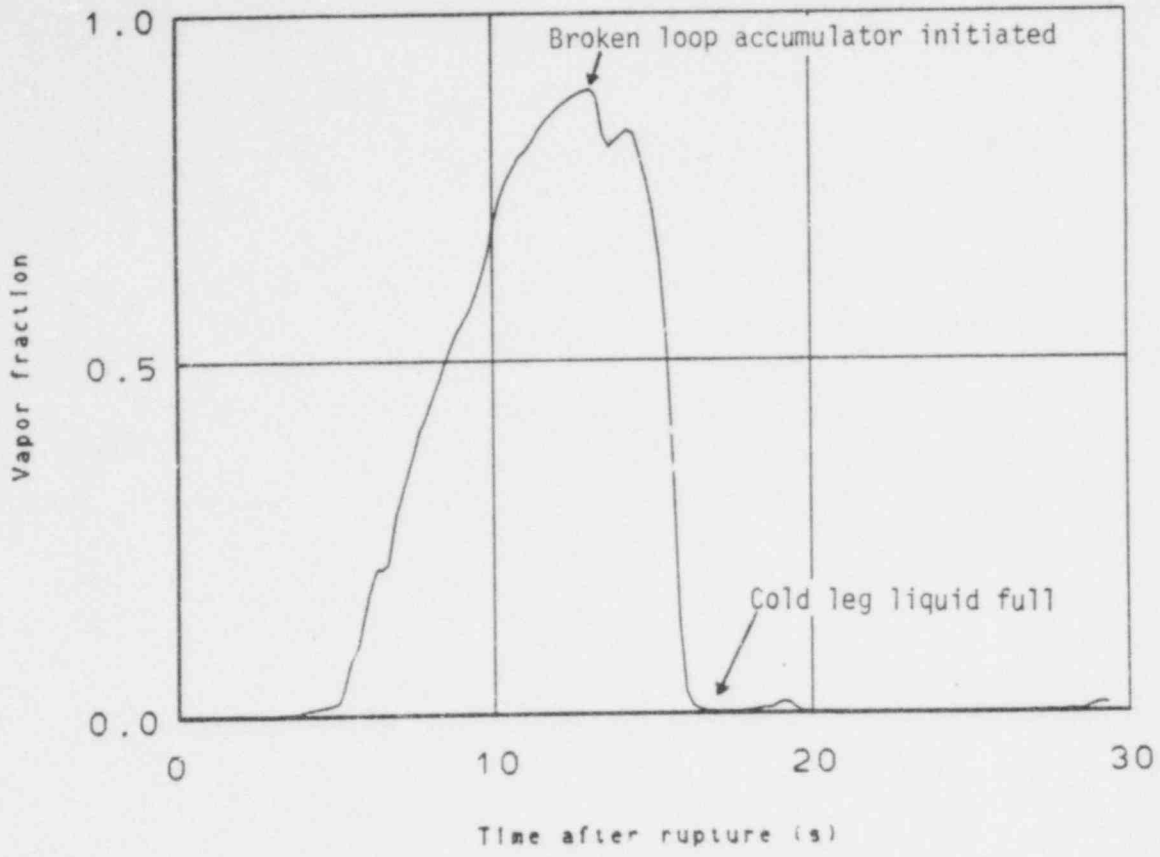

Figure 6. Broken loop (Loop 1) cold leg vapor fraction.

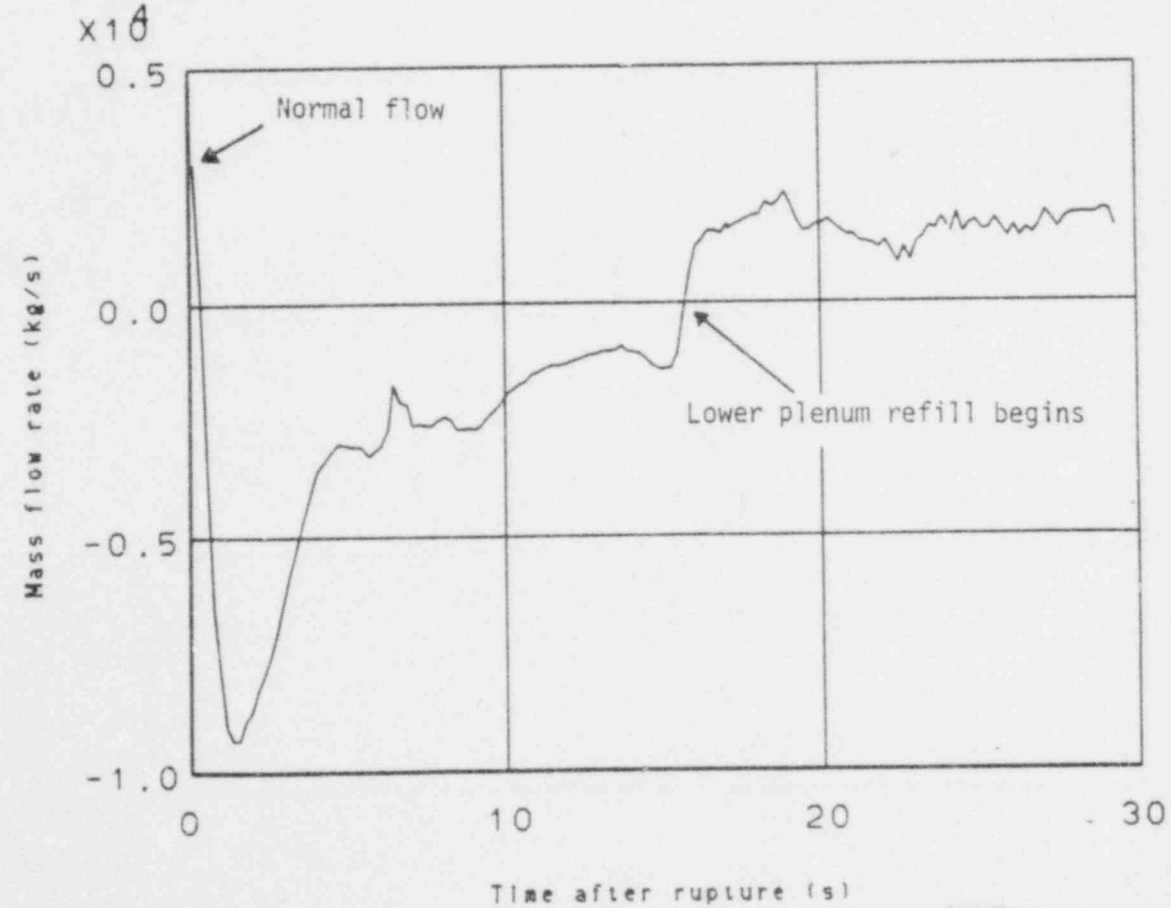

Figure 7. Broken loop (Loop 1) cold leg mass flow rate.

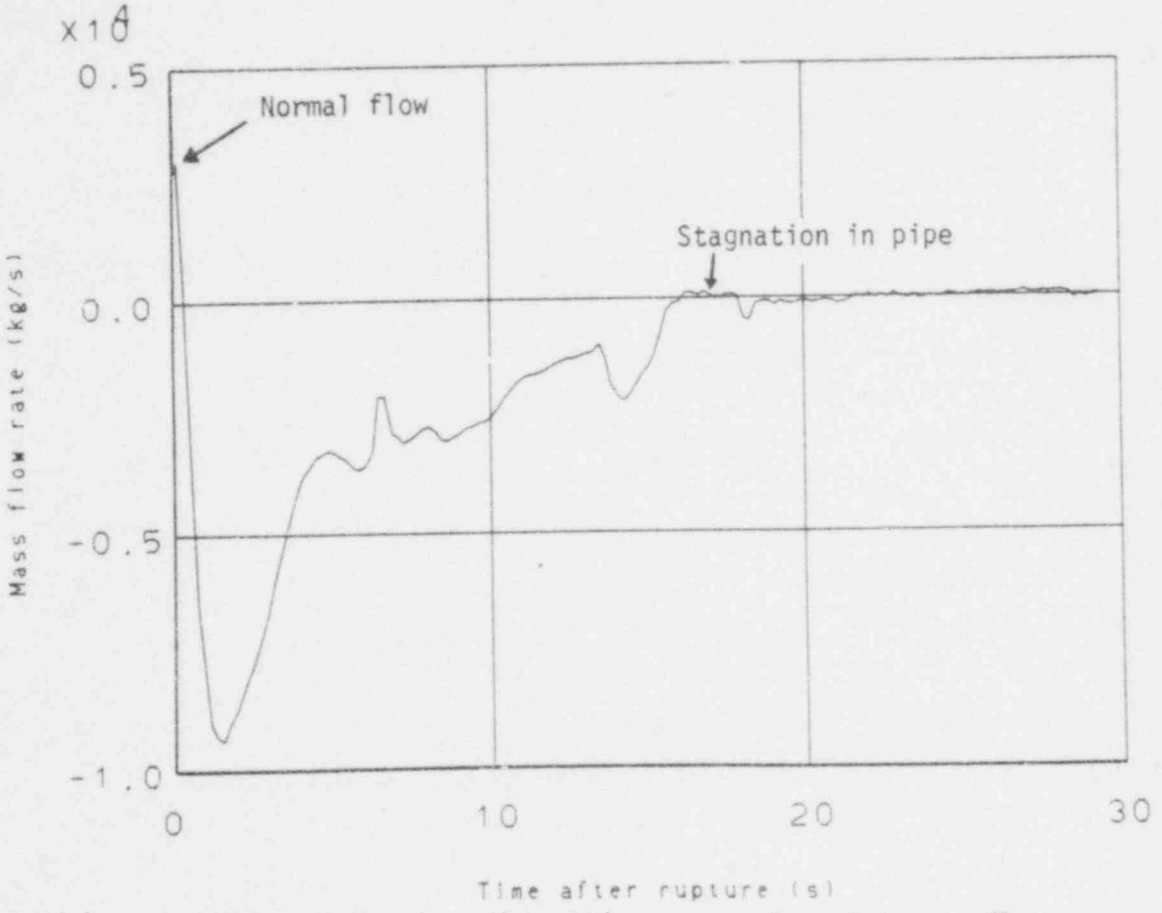

Figure 8. Broken loop (Loop 1) pump suction pipe mass flow rate.

quenched the rods. Some of the two phase mixture generated during core reflood entered the hot leg of the intact loops and traversed around the loops. The remaining two phase mixture exited through the vessel-side break in loop 1, increasing the mass flow rate as seen in Figure 4.

Loops 2 and 3 have nearly identical system behavior; since loop 2 is the loop with the tube rupture in the steam generator tube rupture calculation it will be discussed for the hot leg break calculation.

Until 8.2 s the behavior of the loop 2 hot leg was similar to that of the broken loop hot leg with the exception that the loop 2 flow continued in the normal flow direction as shown in Figure 9. At 8.2 s the steam generator secondary became a heat source to the primary fluid. Figure 10 shows the liquid temperature response of cell 3 of the primary side and cell 2 of the secondary side of the (loop 2) steam generator. This response was similar throughout the steam generator. As the system pressure continued to decrease the primary to secondary temperature differential became larger. Void fractions at the top of the tube bundle in the steam generator primary side approached one, cutting off the two phase circulation and reversing the flow in the hot leg pipe at 10 s as seen in Figure 9. The flow remained reversed for the next 10 s as the void fraction in the hot leg approached one at 20 s as shown in Figure 11. By 20 s the core had begun to reflood, generating a two phase mixture in the core. The amount of two phase mixture generated was more than could exit the break; therefore, the remainder of the two phase mixture being generated began flowing into the hot legs of the loops as seen in Figure 9. From 20 s to the termination of the calculation, the flow in the loop was in the normal direction.

The flow in the cold leg section of loop 2 remained positive except for a short duration around 17 s which will be discussed later. For the first 3 s the flow in the cold leg was nearly constant as seen in Figure 12. As the vessel upper plenum voided, the two phase mixture began flowing through the intact loops as indicated by the vapor fraction of the cold leg in loop 2 shown in Figure 13. The steam generator was a heat

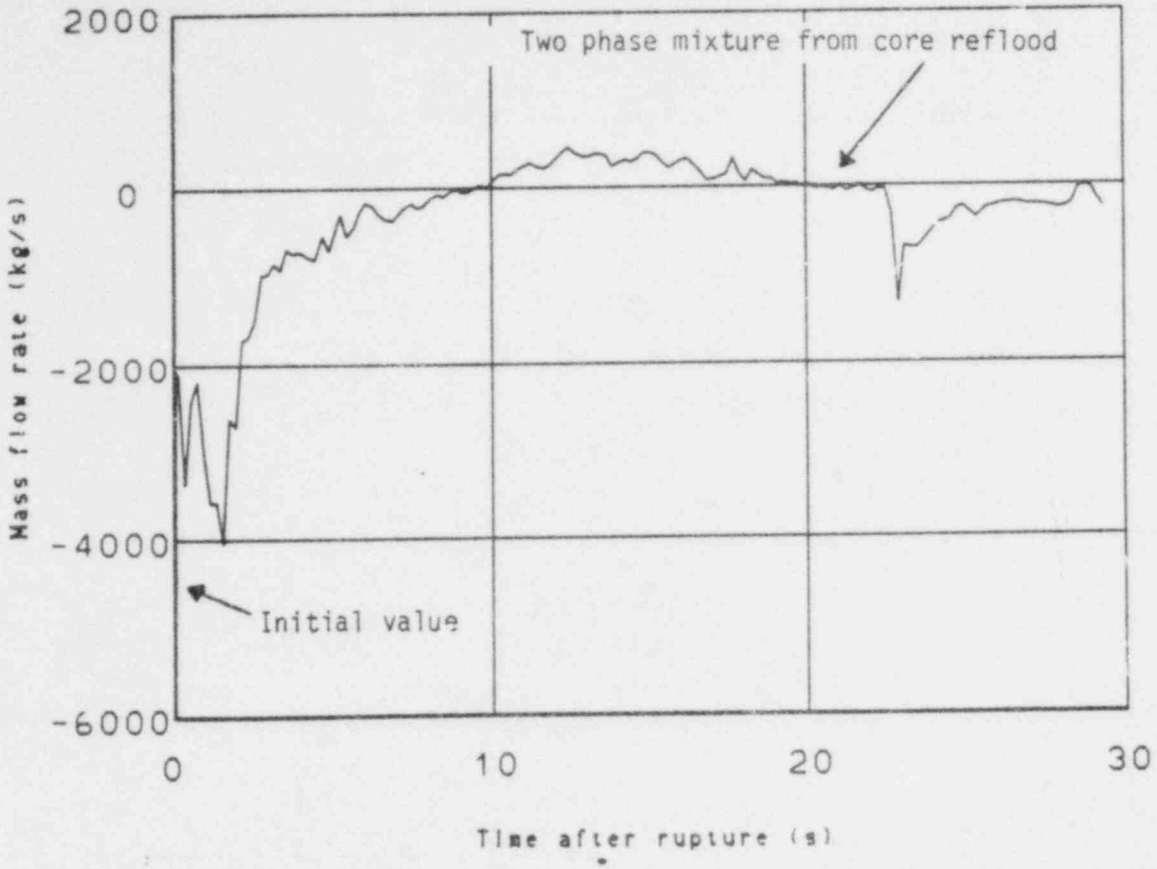

Figure 9. Intact loop (Loop 2) hot leg mass flow rate.

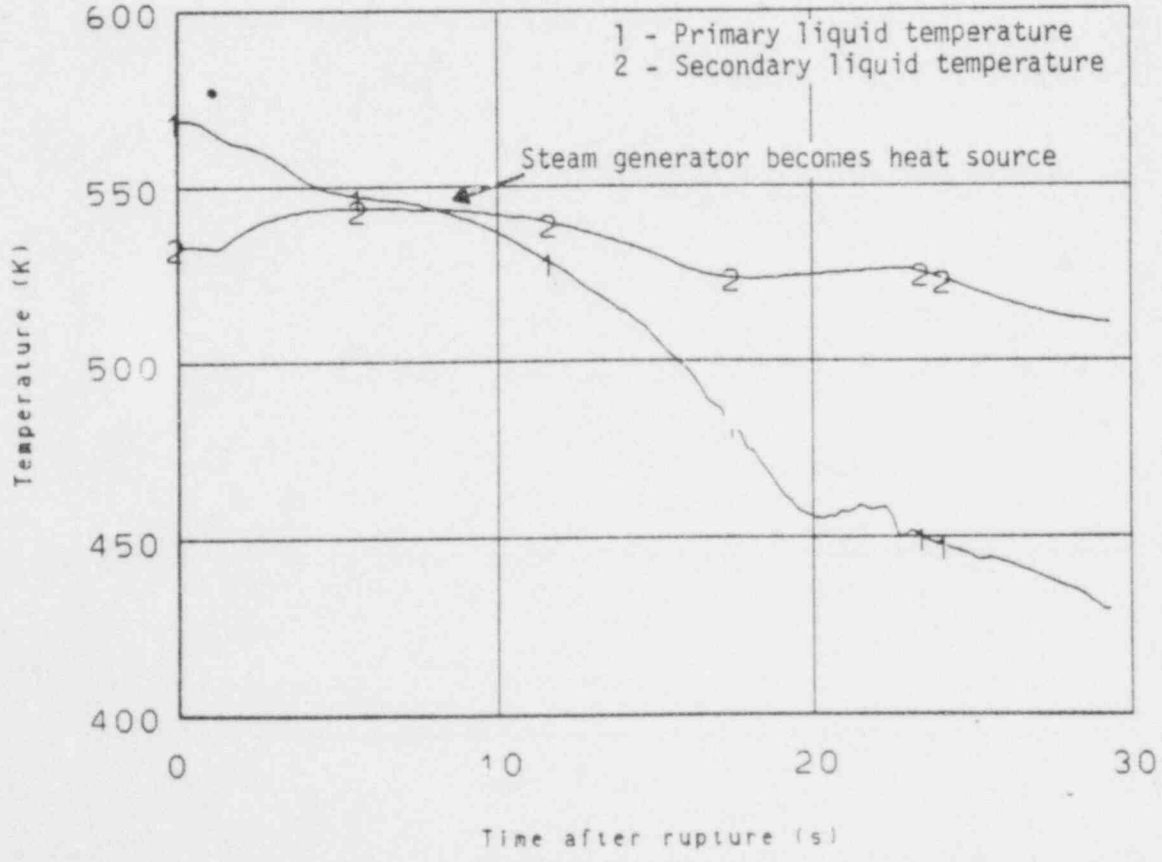

Figure 10. Intact loop (Loop 2) primary-secondary liquid temperature

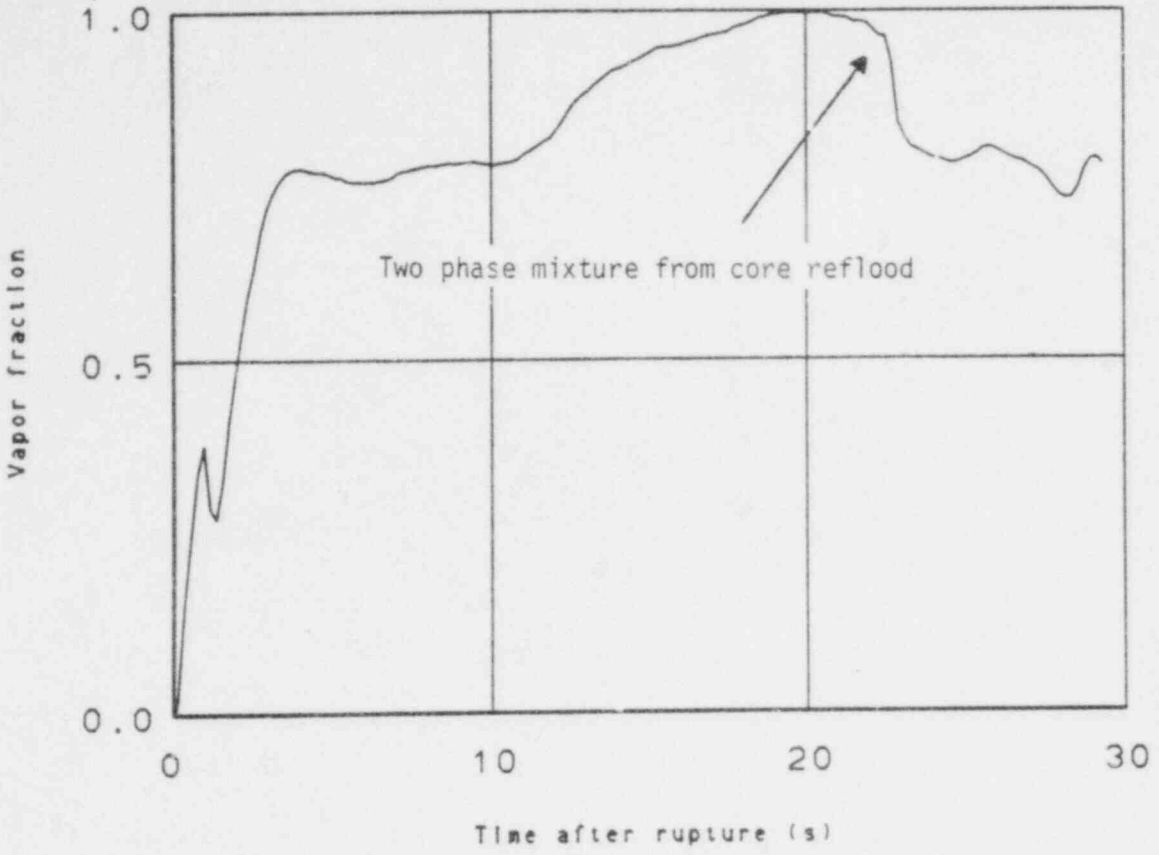

Figure 11. Intact loop (Loop 2) hot leg vapor fraction.

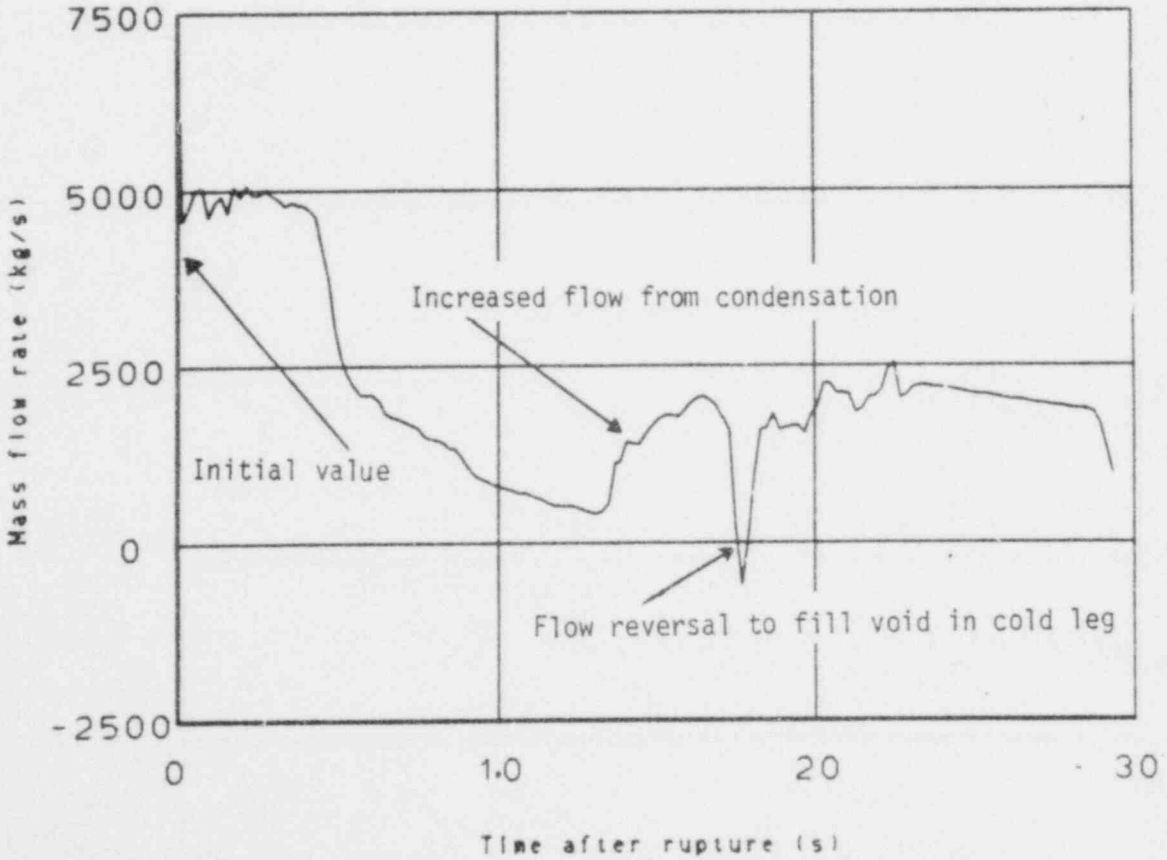

Figure 12. Intact loop (Loop 2) cold leg mass flow rate.

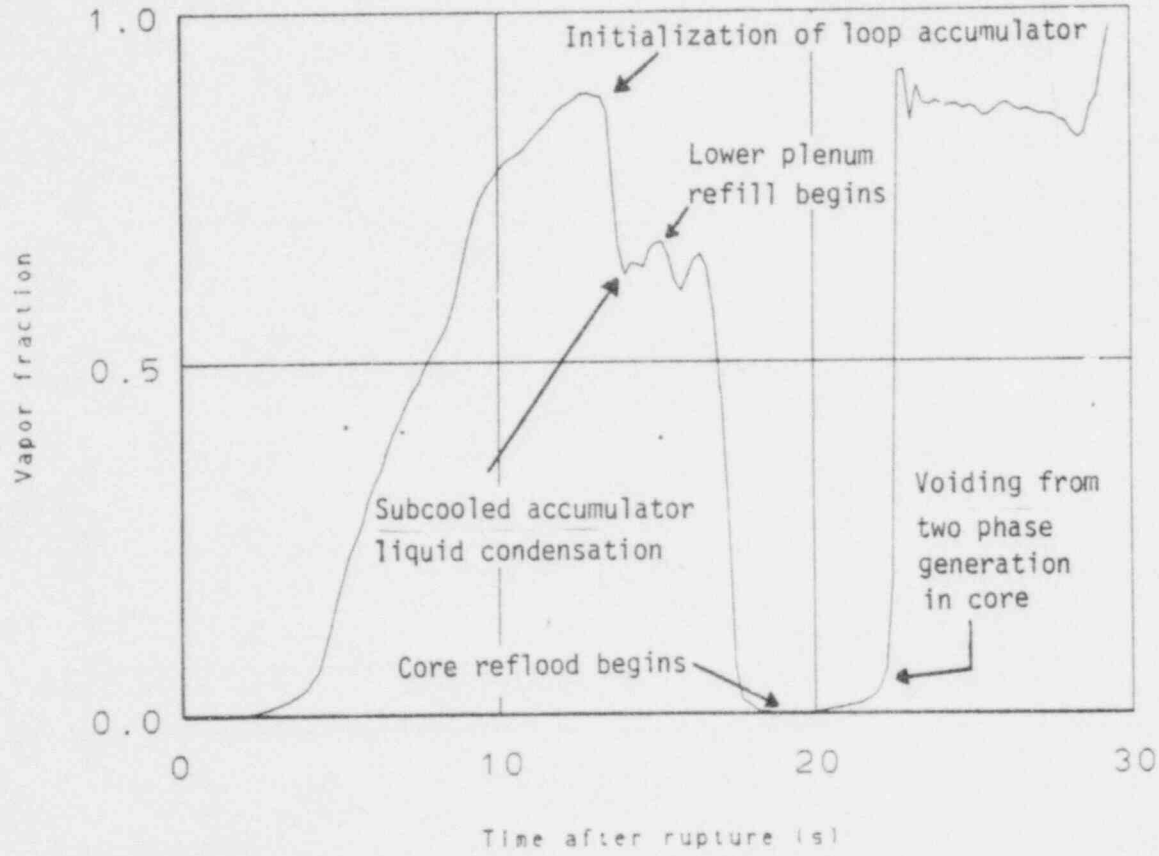

Figure 13. Intact loop (Loop 2) cold leg vapor fraction.

source after 8.2 s and dried out the cold leg side of the steam generator tubes. The pressure differential created from the steam generated in the tubes forced two phase fluid out of the pump suction leg, through the pump and into the cold leg piping.

At 12.56 s loop 2 accumulator injection occurred and began to fill the cold leg pipe. TEE 16 (see Figure 1) was modeled with two primary cells; cell 1 next to the pump and cell 2 connected to the accumulator injection line. The cells from the accumulator injection point to the vessel filled with liquid first because of the direction and momentum of the fluid at the time of accumulator initiation. Condensation took place as the fluid from the accumulator entered the primary loop. The mass flow in the loop increased due to the localized pressure drop from the condensation shown in Figure 12. When the primary cells of TEE 17 and cell 2 of TEE 16 were essentially liquid full the flow reversed momentarily to fill cell 1 of TEE 16 as seen in Figure 12. The cell quickly filled. Some of the liquid penetrated part way through the pump but was unable to go completely through because of the positive pump head. The cold leg mass flow again became positive and continued to inject into the vessel downcomer.

At the time the cold leg of loop 2 became liquid full (18 s) the core had begun to reflood. Almost immediately small amounts of void appeared in the cold leg near the pump. This void came from the pump which was pumping steam at this time. At 20 s the two phase mixture from core reflood entered the hot leg of loop 2. The two phase fluid traversed around the steam generator and was evaporated, increasing the velocity of the vapor. The increased vapor velocity and the positive pump head pushed the liquid in the cold leg near the pump to the cold leg near the vessel connection and into the inlet annulus. The accumulator and HPIS/LPIS fluid continued to inject subcooled liquid into the cold leg causing condensation which slightly reduced the pressure in the cold leg. The reduction in pressure increased both the accumulator and HPIS/LPIS discharge rate as shown in Figures 14 and 15. At 28.4 s steam from the accumulator was injected into the cold leg. At 28.8 s the accumulator flow was shut off.

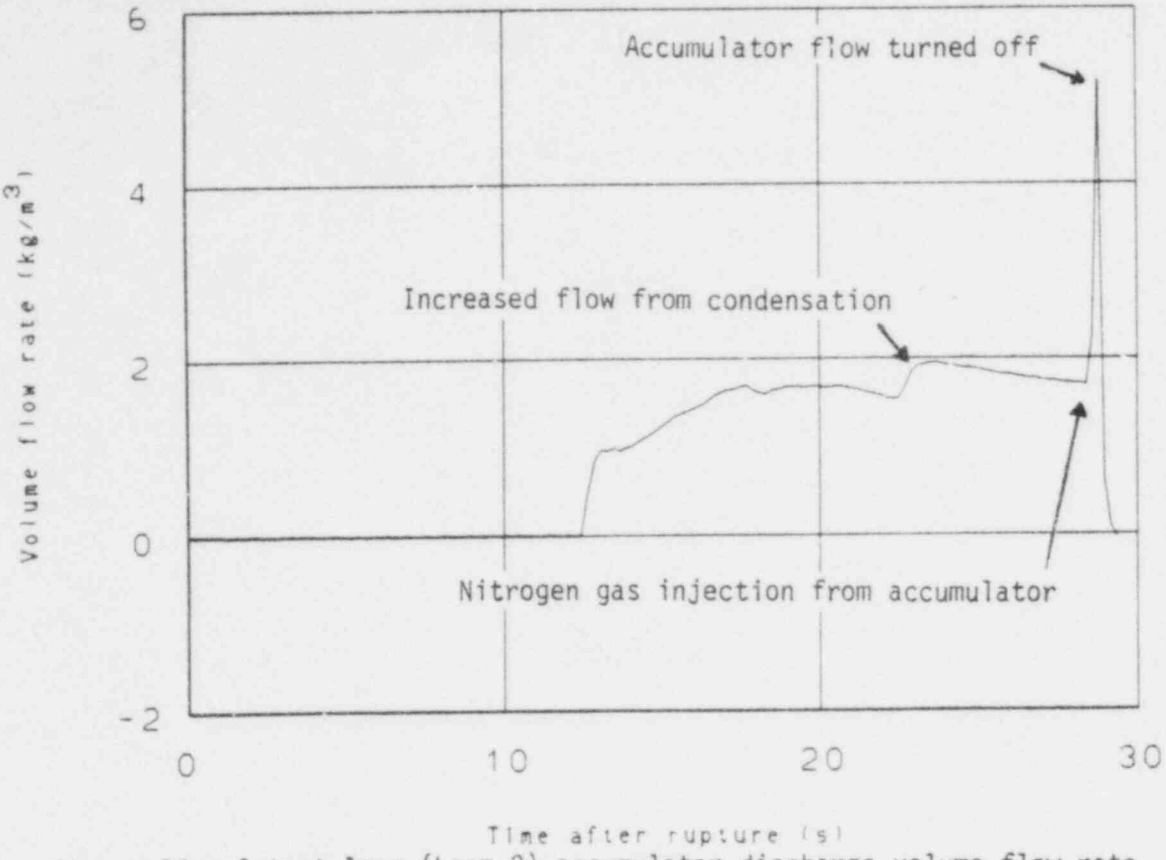

Figure 14. Intact.loop (Loop 2) accumulator discharge volume flow rate.

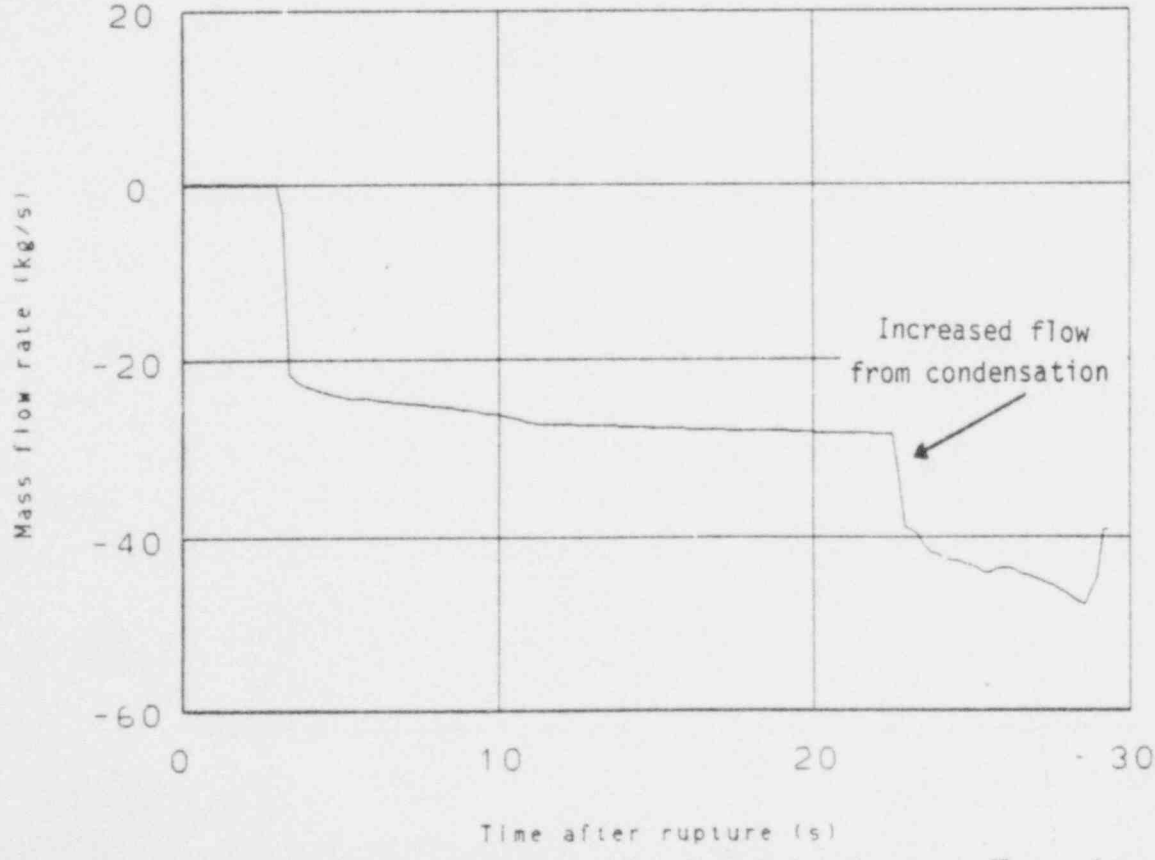

Figure 15. Intact loop (Loop 2) safety injection mass flow rate.

The behavior in loop 4 was similar to loop 2 with the exception of the hot leg response. The hot leg of loop 4 had the pressurizer attached to it.

At the initiation of the break, the depressurization of the pressurizer lagged the depressurization of the system for the first 14 s as seen in Figure 16. The pressure differential forced fluid out of the pressurizer and pressurizer surge line into the hot leg. The fluid split, part of it going into the upper annulus of the vessel and the remainder going around the loop. Figure 17 shows the flow in the hot leg (loop 4) near the vessel reversing, flowing into the upper annulus until 18.8 s. The rest of the fluid in the hot leg continued to flow around the loop until 10 s as seen in Figure 17.

From 8 s to the end of the calculation the behavior in loop 4 was quite similar to that of loop 2. The steam generator acted as a heat source, drying out the fluid in the primary tubes and caused the flow in the hot leg side of the steam generator tubes to reverse direction. At 12.6 s the accumulator came on. At 18.6 s the flow in the hot leg reversed direction and began flowing in the normal direction because of two phase mixture generated in the core due to core reflood. The pressurizer was empty at 21.2 s and the accumulator was shut off at 27.8 s.

The vessel thermal-hydraulic behavior will be discussed next. Asymmetric effects during blowdown will be discussed followed by a discussion of the core behavior during the calculation.

During blowdown, asymmetric effects were seen in the vessel as the liquid exited the break. In the downcomer the liquid axial flow was down the downcomer except in the cell connecting the broken loop (cell 18) which was up the downcomer as shown in Figure 18. In the core the axial flow was always positive as indicated by the core inlet flow in Figure 19. Figure 20 depicts the direction of the radial and tangential liquid velocities in vessel level 9 at 10 s which was typical during the course of blowdown. The magnitude of the radial and tangential velocities was between 2 and 10 m/s.

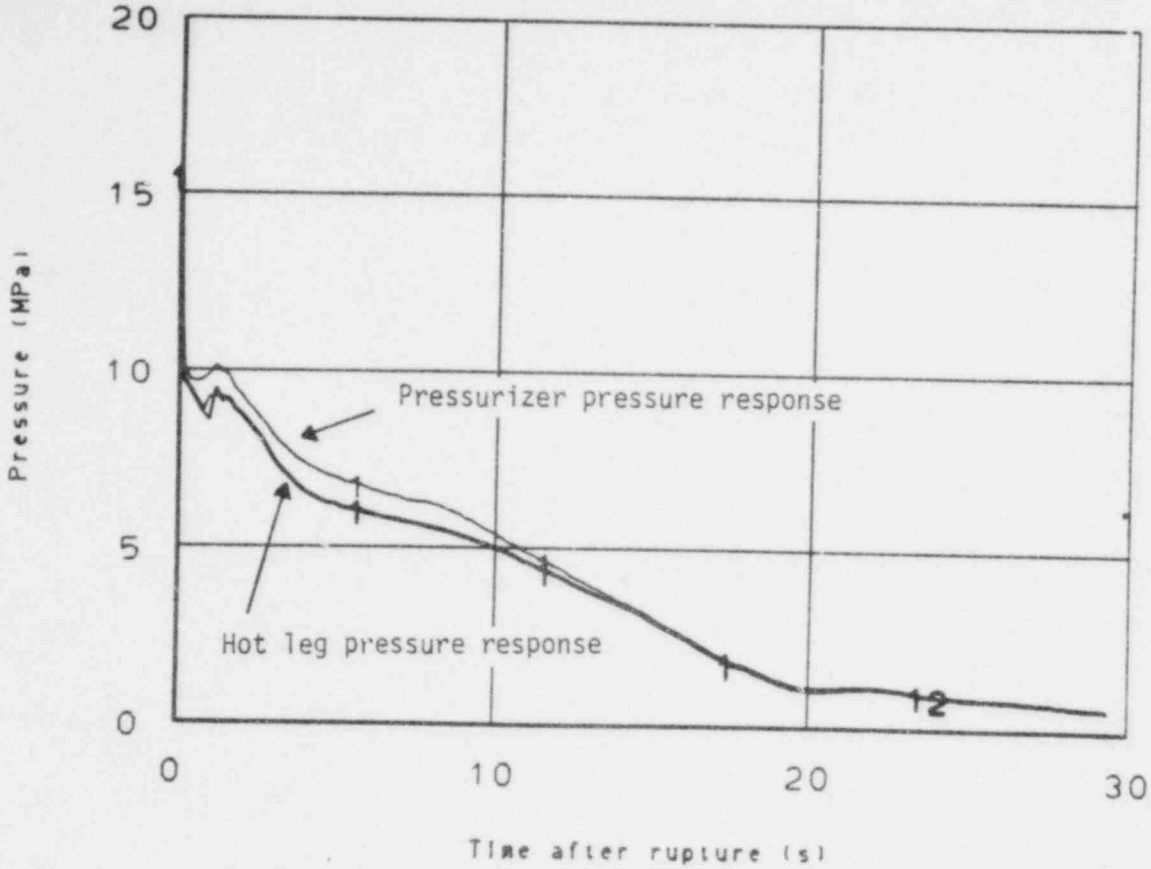

Figure 16. Intact loop (Loop 4) hot leg pressure.

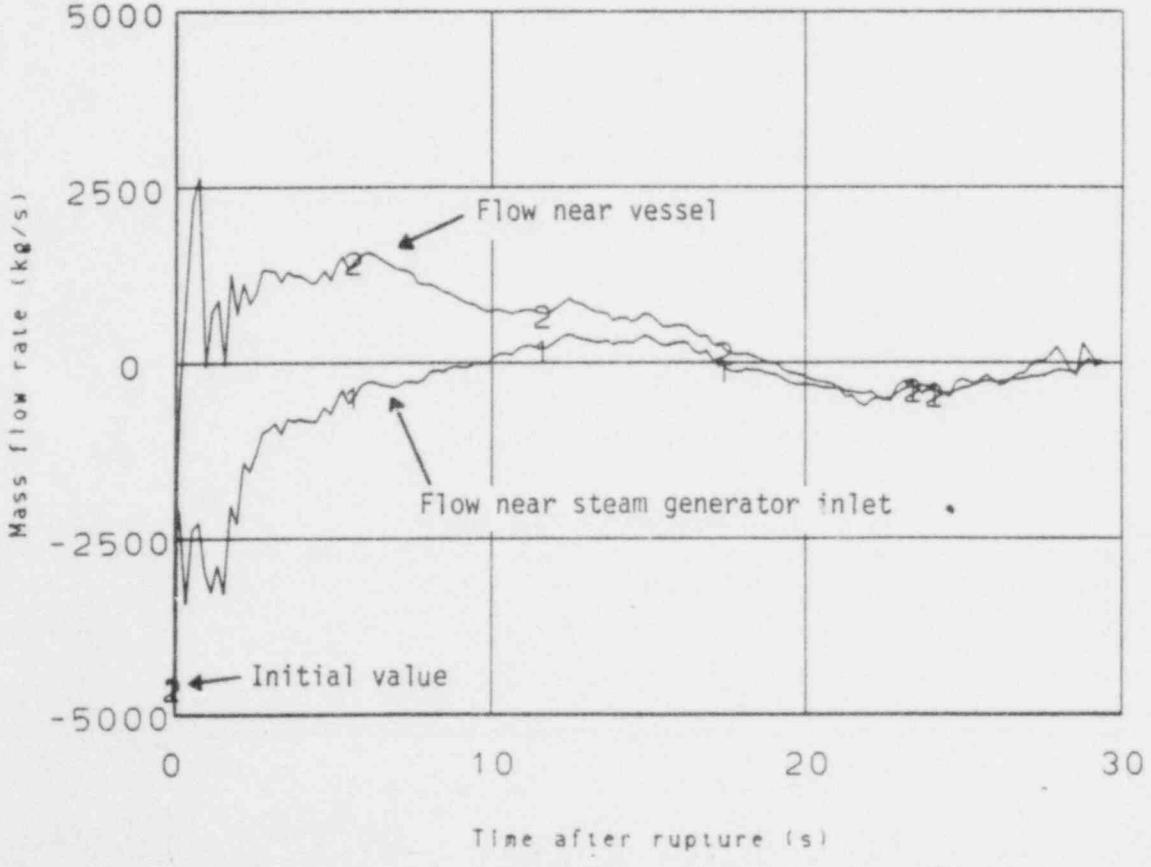

Figure 17. Intact loop (Loop 4) hot leg mass flow.

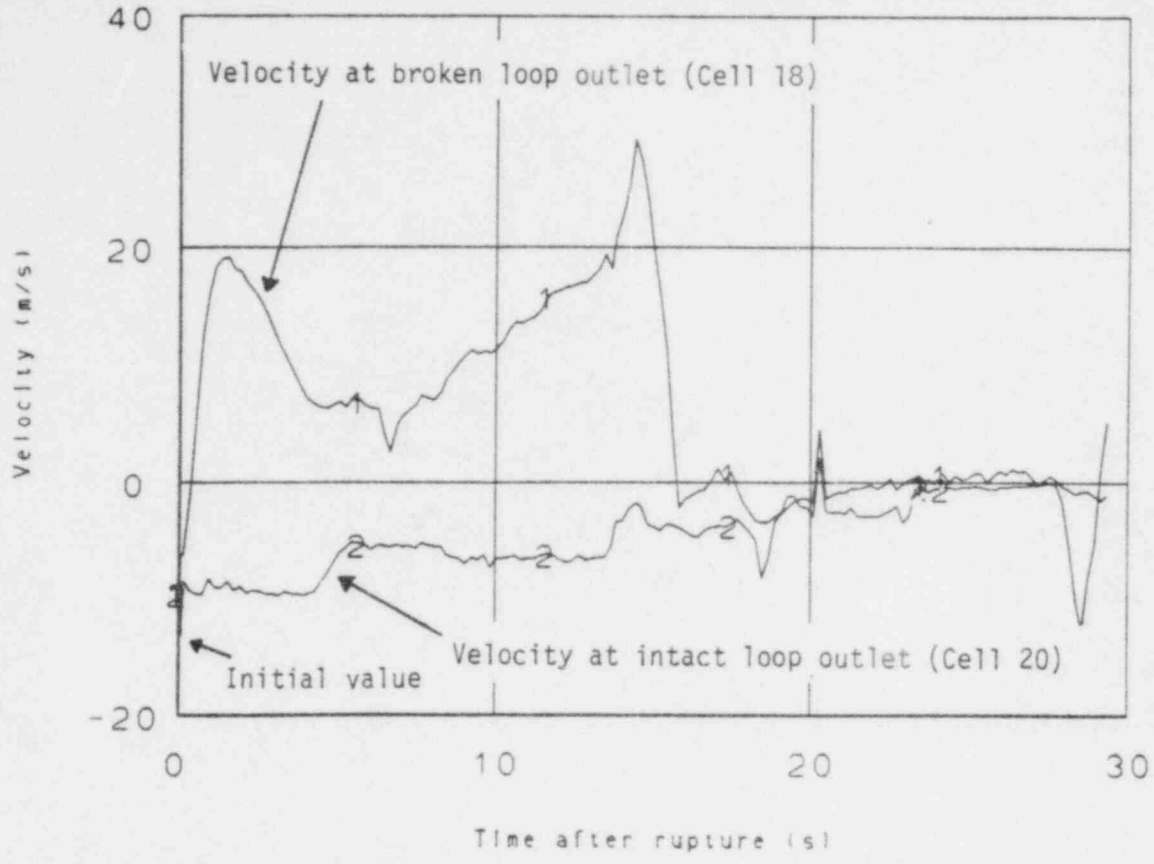

Figure 18. Vessel downcomer axial liquid velocity.

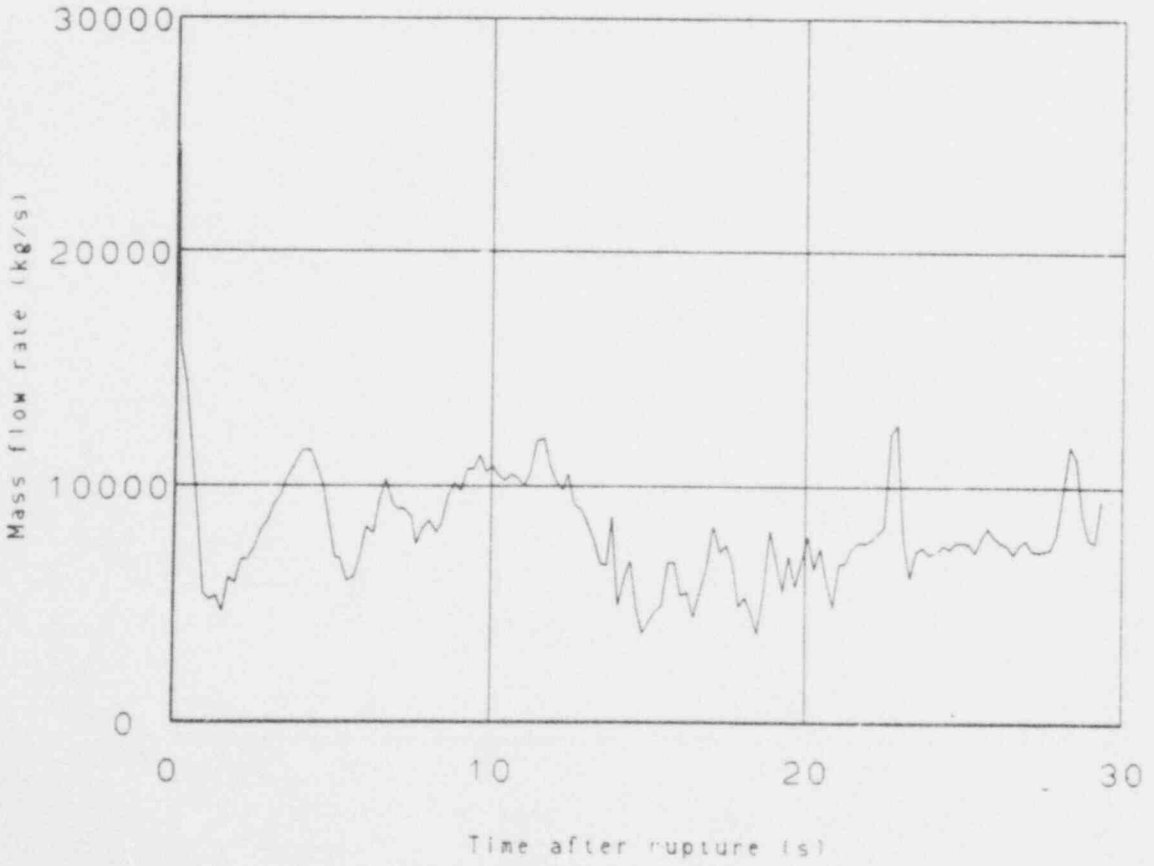

Figure 19. Vessel core inlet mass flow.

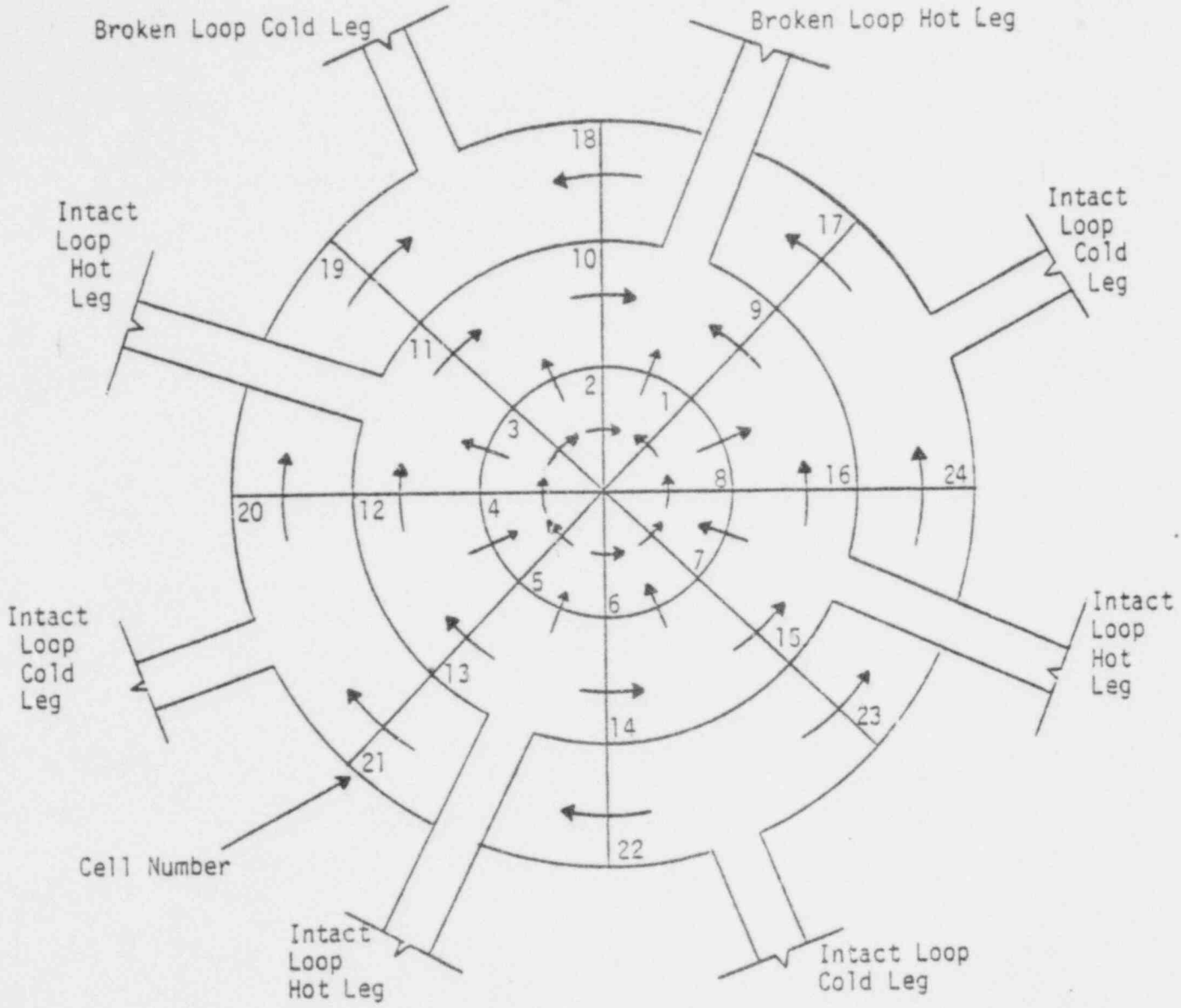

Figure 20. Radial and azimuthal liquid velocity direction.
Vessel level 9 at 10 sec.

The vessel first began voiding in the upper plenum, then voiding traversed down through the core section and into the lower plenum as indicated in Figures 21 and 22.[a] The upper head voided due to loss of liquid in the upper plenum, depressurization and gravitational effects. Void in the downcomer increased as liquid from the downcomer flowed into the core to replace the core void. Voiding was also induced in the downcomer region as fluid exited through the cold leg piping of the broken loop. At 14 s the accumulators and HPIS/LPIS were injecting liquid into the downcomer. The effects of the injection were seen in the lower section of the downcomer and lower plenum by the decrease in the void fraction as seen in Figure 23.[b] By 15 s the core was essentially void. At 15.6 s refill had begun as indicated in Figure 24. The liquid from the HPIS/LPIS and accumulator systems began to penetrate the downcomer and lower plenum. At 18.6 s the downcomer and lower plenum was 70-85% liquid full and two phase fluid began to reflood the core. The liquid in the downcomer provided the head necessary for the core to reflood. During core reflood it was noted that the core did not reflood with a constant liquid level in each cell. The stack of vessel azimuthal sections connected to the break remained void longer than the other cells in the core until 19-20 s, at which time core reflood became more uniform. The cause of the high vapor fractions in the azimuthal sections connected to the break cannot be explained at this time. Further investigation into this phenomenon should be conducted. By 21.2 s the downcomer was almost liquid full creating a larger head and allowing the core to reflood at a faster rate. By 25.5 s the core had refilled.

---

a. Figures 21 and 22 are azimuthal cuts through the vessel. One taken through the broken loop hot leg section and the other taken through the broken loop cold leg section.

b. Figure 23 shows only four of the 8 downcomer azimuthal cells. The four cells not shown behave similarly to those of cells 20 and 22.

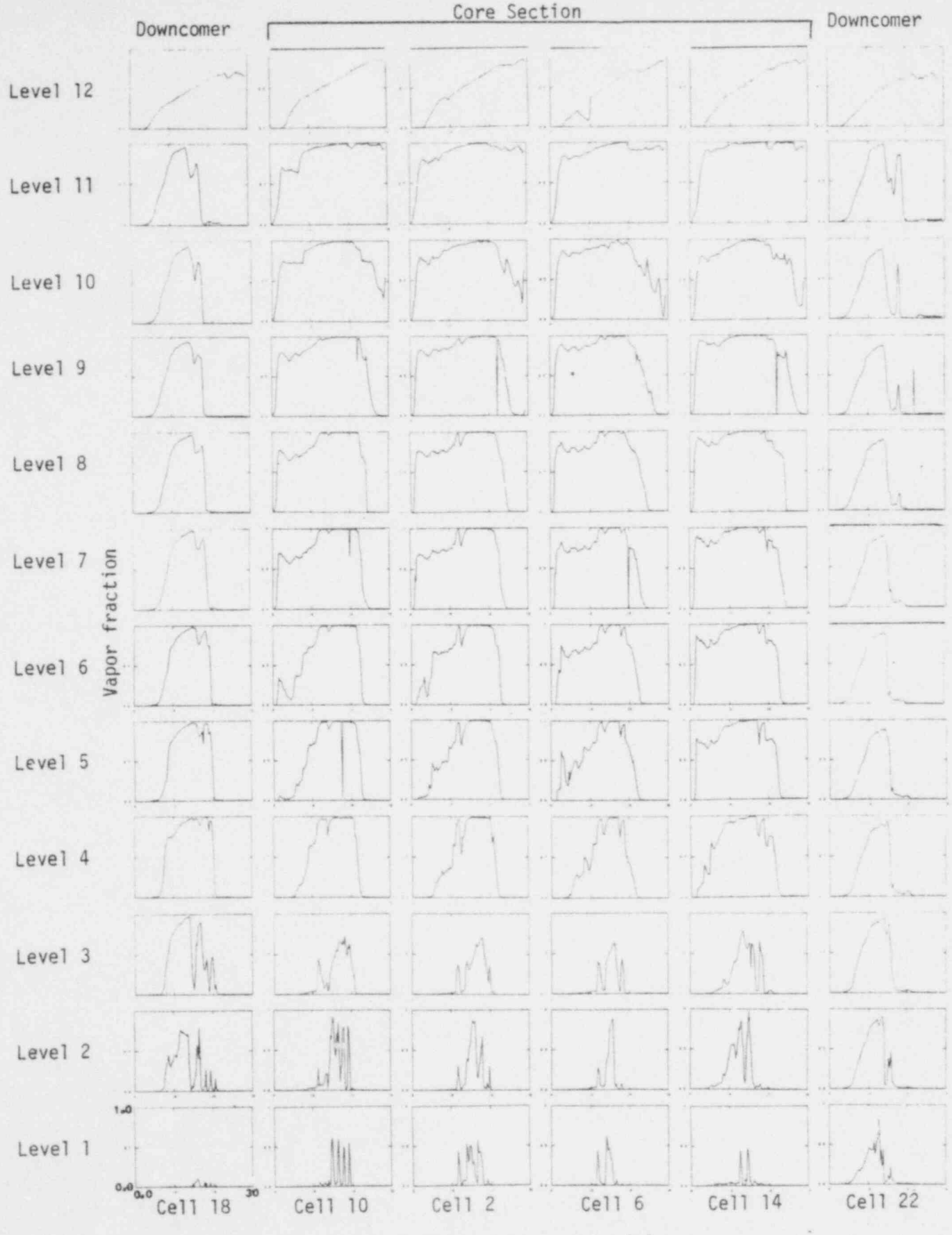

Figure 21. Vapor fractions of vessel theta section cutting through the broken loop hot leg connection.

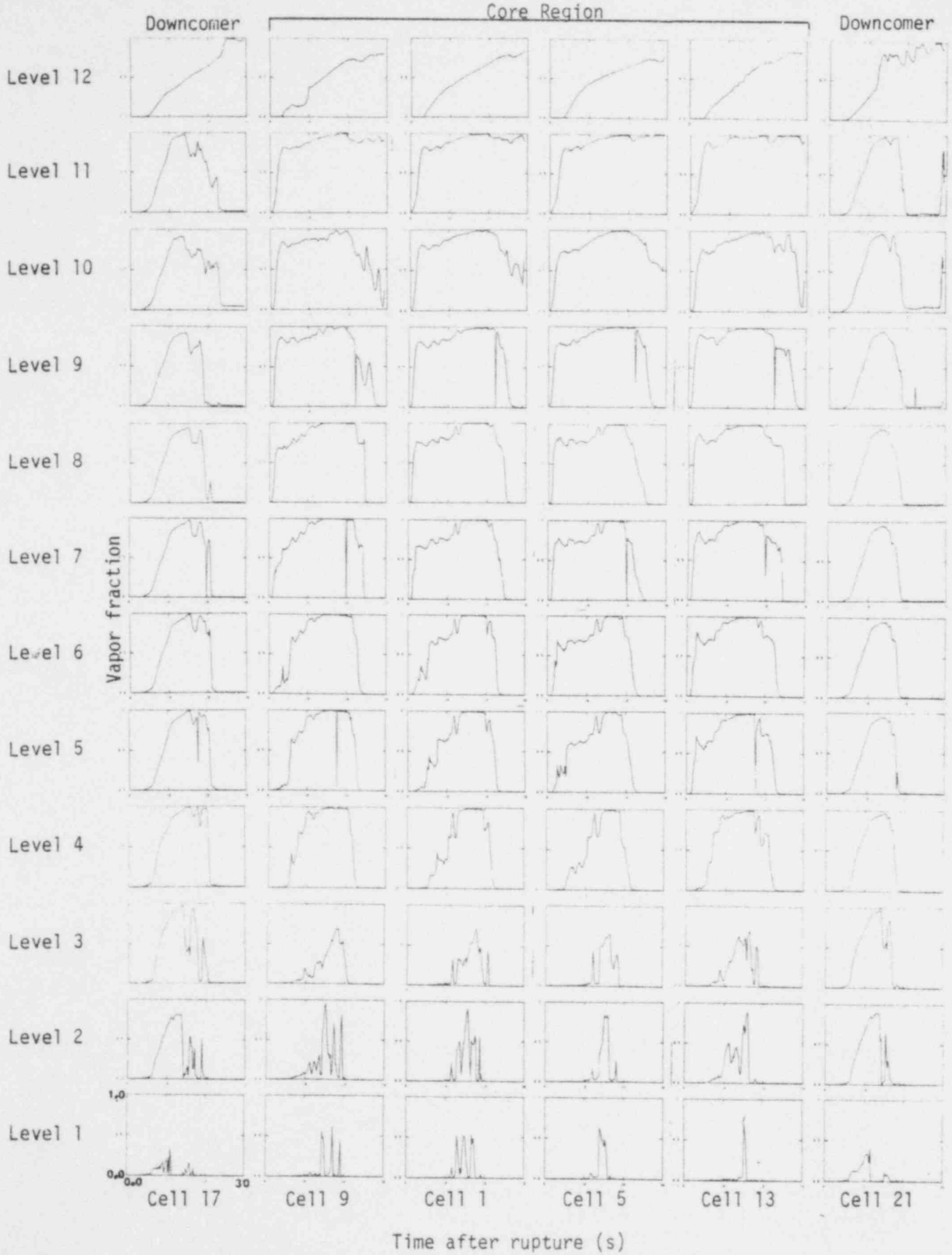

Figure 22. Vapor fraction of vessel theta section cutting through the broken broken loop cold leg connection.

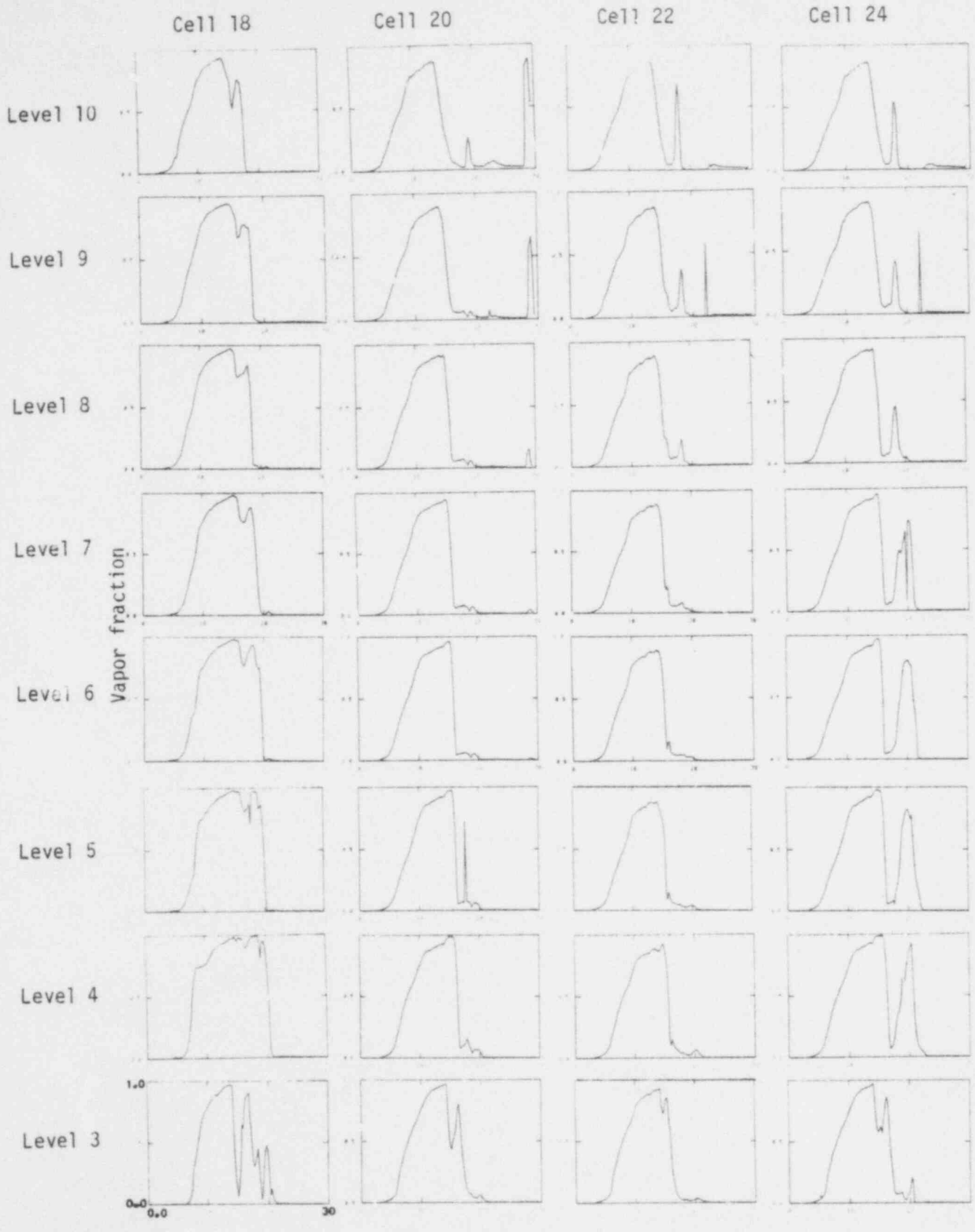

Figure 23. Void fraction of unwrapped vessel downcomer.

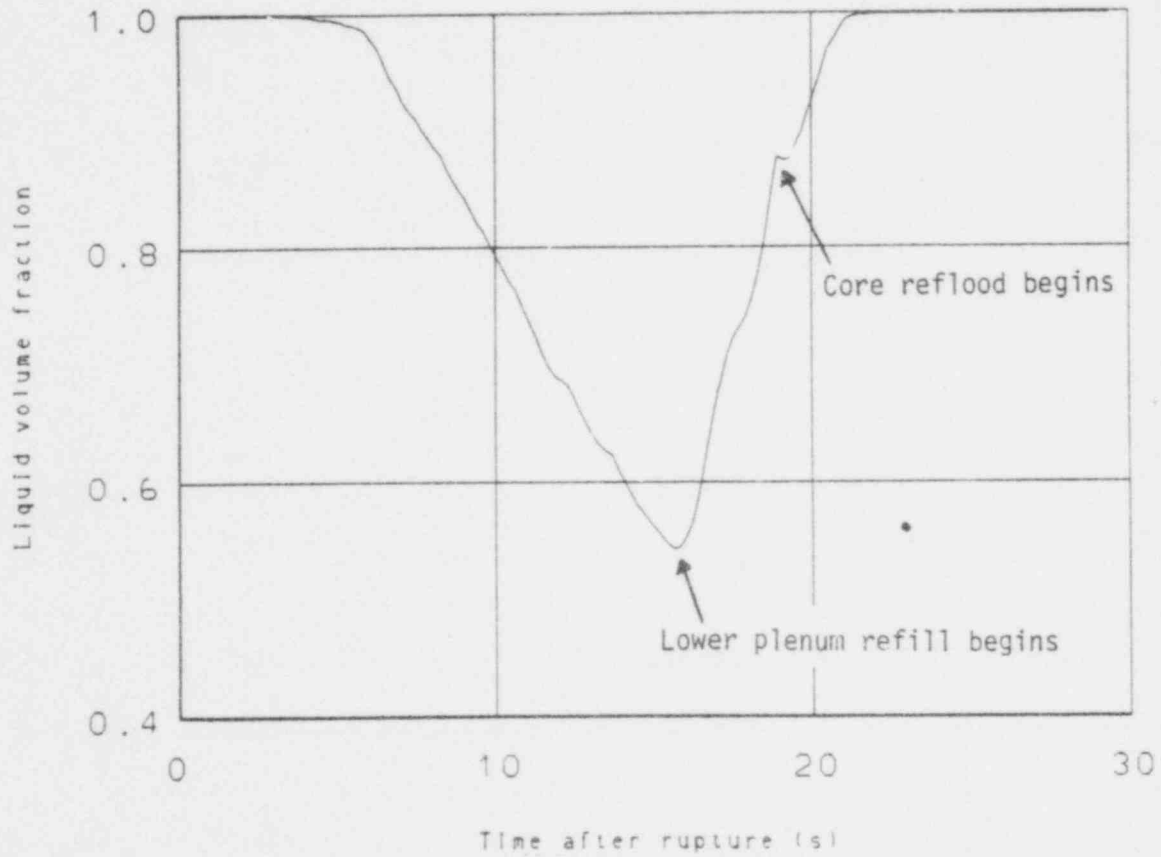

Figure 24. Vessel lower plenum liquid volume fraction.

During the first 1.5 s the liquid in the core experienced a 20 K superheat caused by the rapid system depressurization. The liquid then flashed to steam increasing the system pressure, retarding the core flow and creating a void in the core which caused an increase in the rod clad temperatures as indicated in Figure 25. The system continued to blow down and core flow increased providing sufficient cooling to the rods to decrease the clad temperatures. At 15.6 s the core was essentially void and the rod clad temperatures began to increase. Core reflood began at 18.6 s with a two phase mixture and some rods began to quench. By 20 s all of the rods had begun to quench. As the rods quenched, the liquid level in the core increased. At 21.2 s an increase in core reflood rate occurred due to the larger head in the downcomer and the rod clad temperatures rapidly decreased as seen in Figure 25. Throughout the calculation the rods never exceeded temperatures of 644 K because of sufficient cooling from the positive core flow. The rods had completely quenched by 22 s.

A comparison of the TRAC hot leg break calculation to a Semiscale hot leg break test[8] showed good agreement in the general trend of the behavior. The major events during blowdown occurred earlier in the calculation than in the test because of differences in initial conditions and in the two facilities being compared. Different modeling techniques, better agreement on initial conditions and pressure differential in the loops and at the break plane may improve the calculational comparison.

3.3 Steam Generator Tube Rupture Effects

The effects of a steam generator tube rupture on the hot leg break were relatively small. The loop response was similar except in the vicinity around the tube rupture. The vessel behavior was different in that the vapor fractions and clad temperatures remained high longer.

Loop 2 was the loop with the steam tube rupture. The rupture occurred at 0.0 s, concurrent with the large hot leg break, and immediately the fluid from the hot leg began to flow into the steam generator secondary

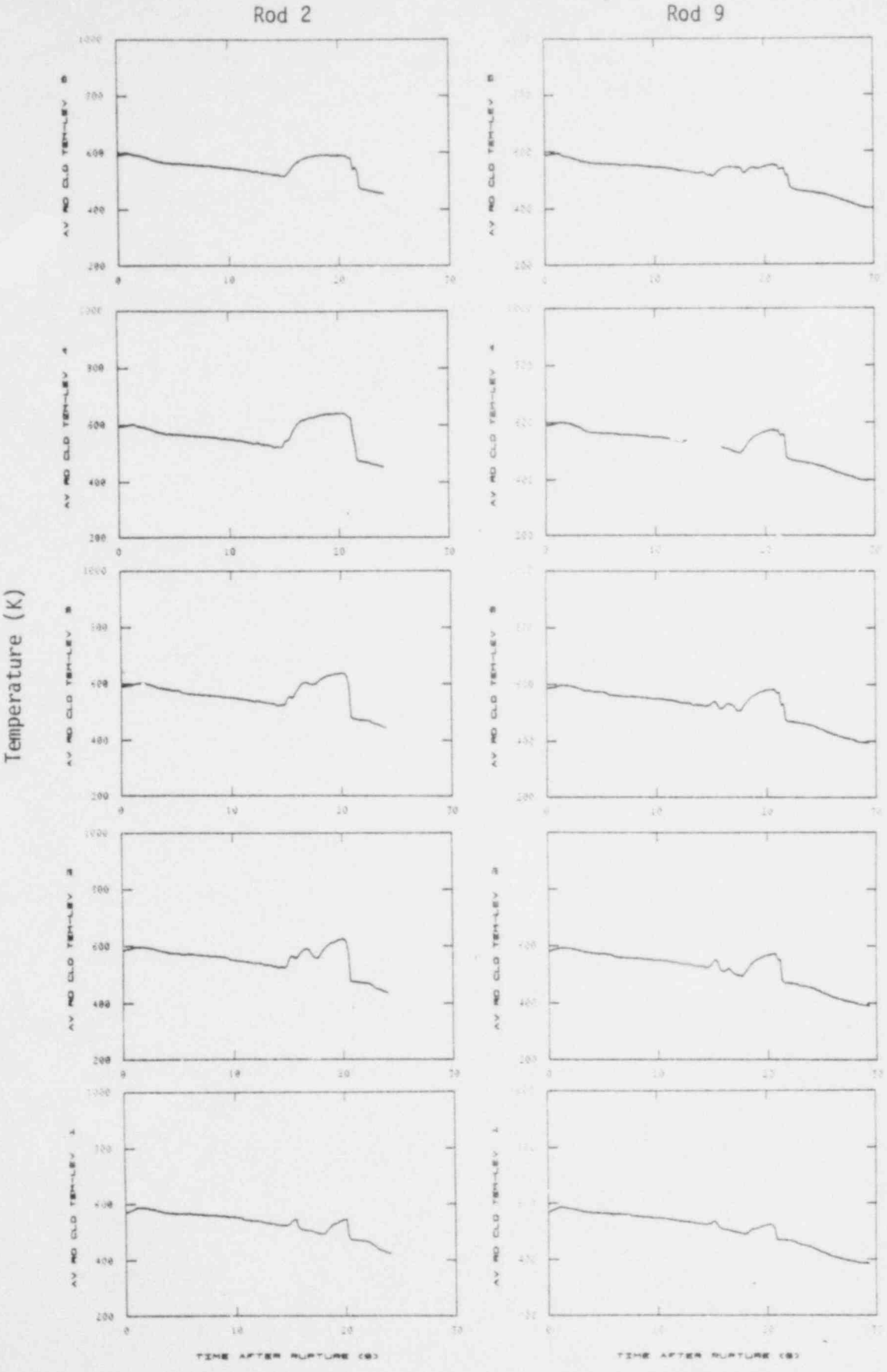

Figure 25. Rod clad temperature profile of rods 2 and 9.

because the primary pressure was higher than the secondary pressure as seen in Figure 26. At 7.8 s the pressure in the loop 2 steam generator secondary was equal to the primary system pressure. The flow reversed and the secondary side fluid began flowing into the primary side as seen in Figure 27. The saturation temperature of the secondary side was higher than on the primary side after 7.8 s because of the pressure differential shown in Figure 27. The steam generator secondary became a heat source because of the temperature difference and dried out the fluid in the steam generator primary tubes. The hot leg reversed flow and began injecting into the vessel upper plenum as was seen in the hot leg break calculation. The liquid from the steam generator secondary tube rupture did not traverse around the loop but flowed into the upper plenum until 23 s when the flow reversed directions as seen in Figure 28.

The loop behavior in the cold leg of loop 2 and the behavior of the other loops was very similar to the hot leg break calculation as shown in Figures 29 through 32.

The vessel response of the steam generator tube rupture was very similar to that of the hot leg break. The 200% break dominated any preferential flow that would have been seen from the tube rupture. The system pressure remained higher in the steam generator tube rupture calculation than in the hot leg break calculation between 20 s and 23.6 s due to a decrease in break mass flow rate. The break mass flow rate was decreased because of an increase in two phase density at the break. At 20 s in the hot leg break calculation the flow in the hot leg in loop 2 had reversed and began flowing in the normal direction as indicated in Section 3.2. However, in the tube rupture calculation, the flow in the hot leg continued to inject secondary liquid into the upper plenum as seen in Figure 28. The liquid traversed around the upper plenum and exited through the break. The increase in liquid at the break increased the two phase density. The higher pressure retarded the core mass flow rate which delayed the beginning of upper core reflood and rod clad quench as seen in

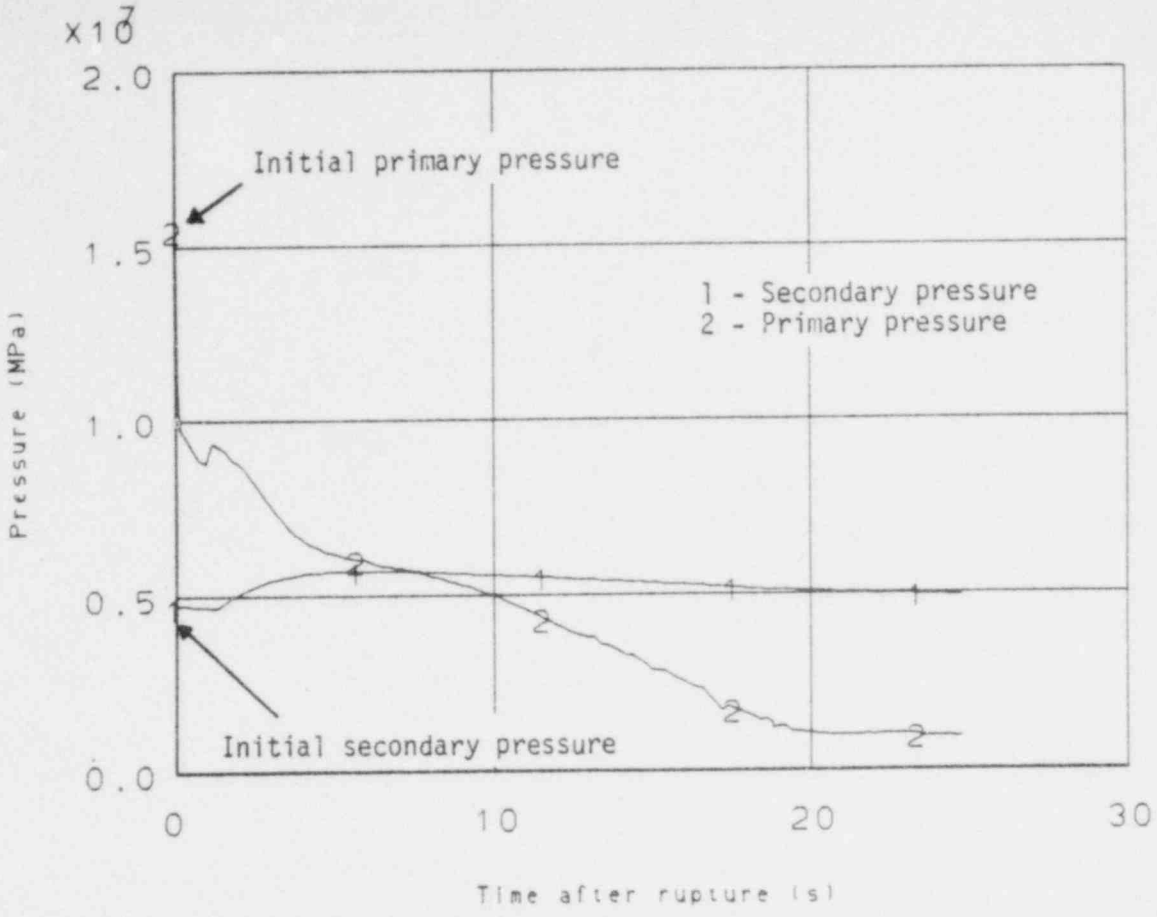

Figure 26. Tube rupture loop (Loop 2) primary-secondary pressure response.

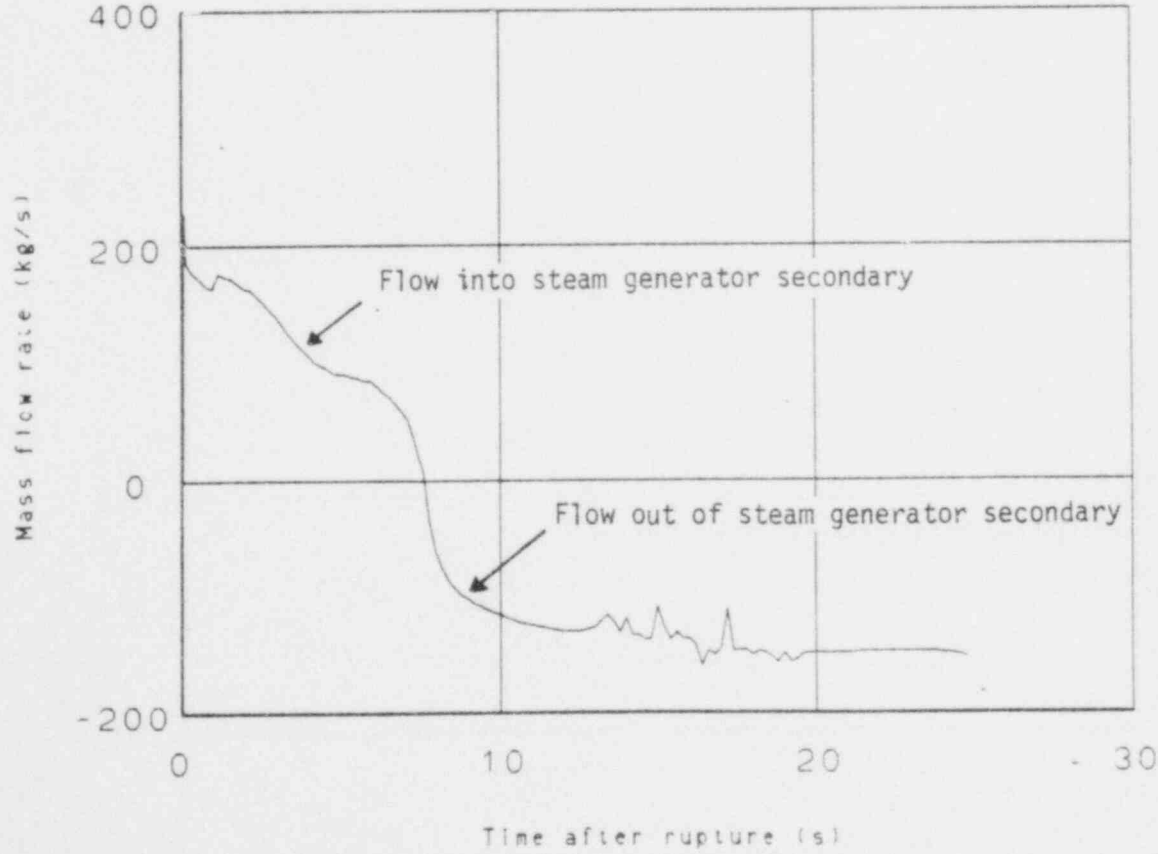

Figure 27. Mass flow of simulated tube rupture.

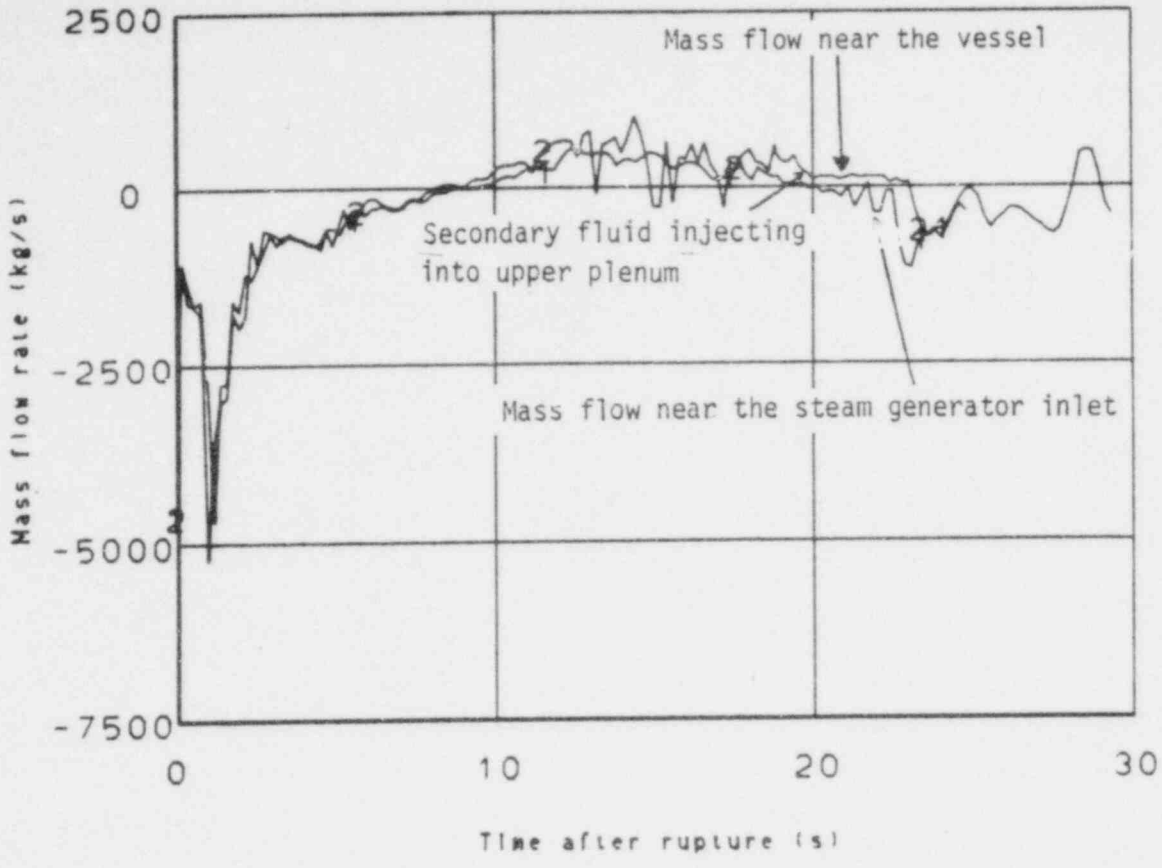

Figure 28. Tube rupture loop (Loop 2) hot leg mass flow rate.

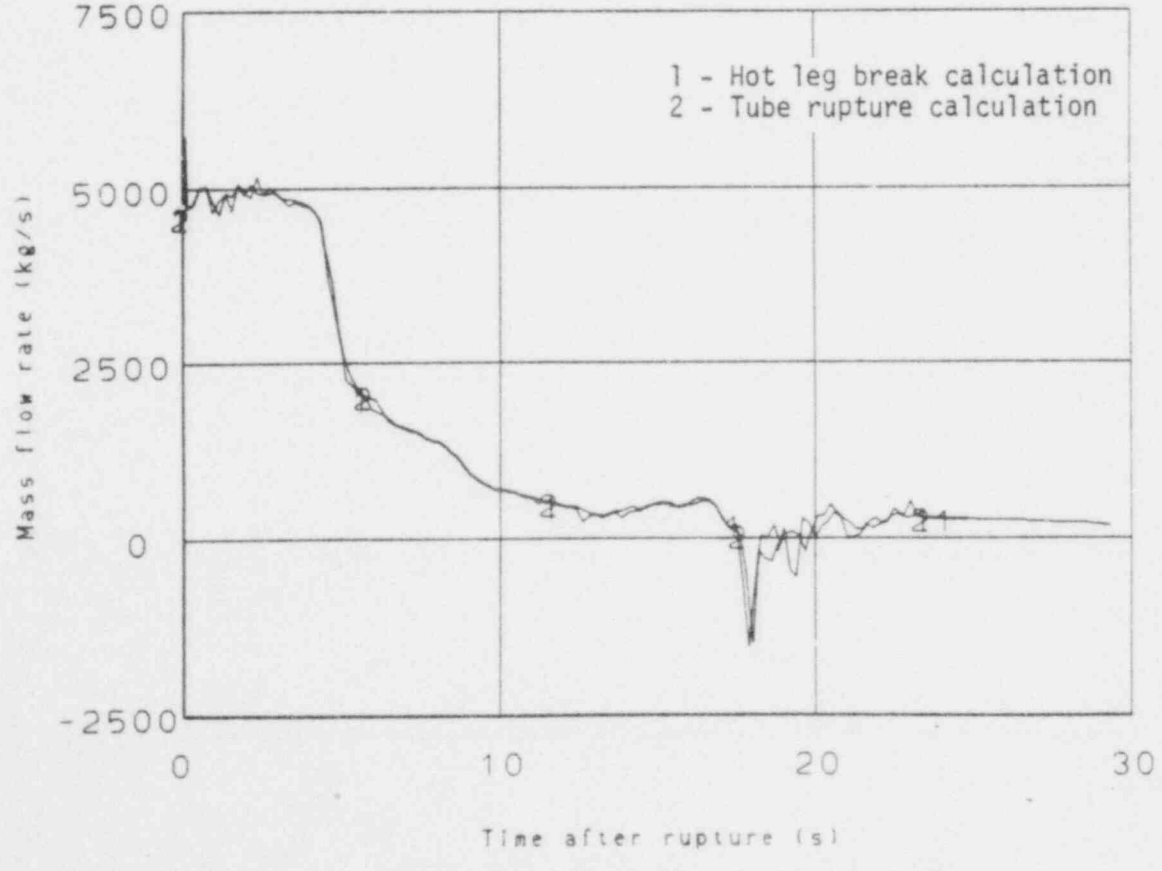

Figure 29. Intact loop (Loop 2) cold leg mass flow rate

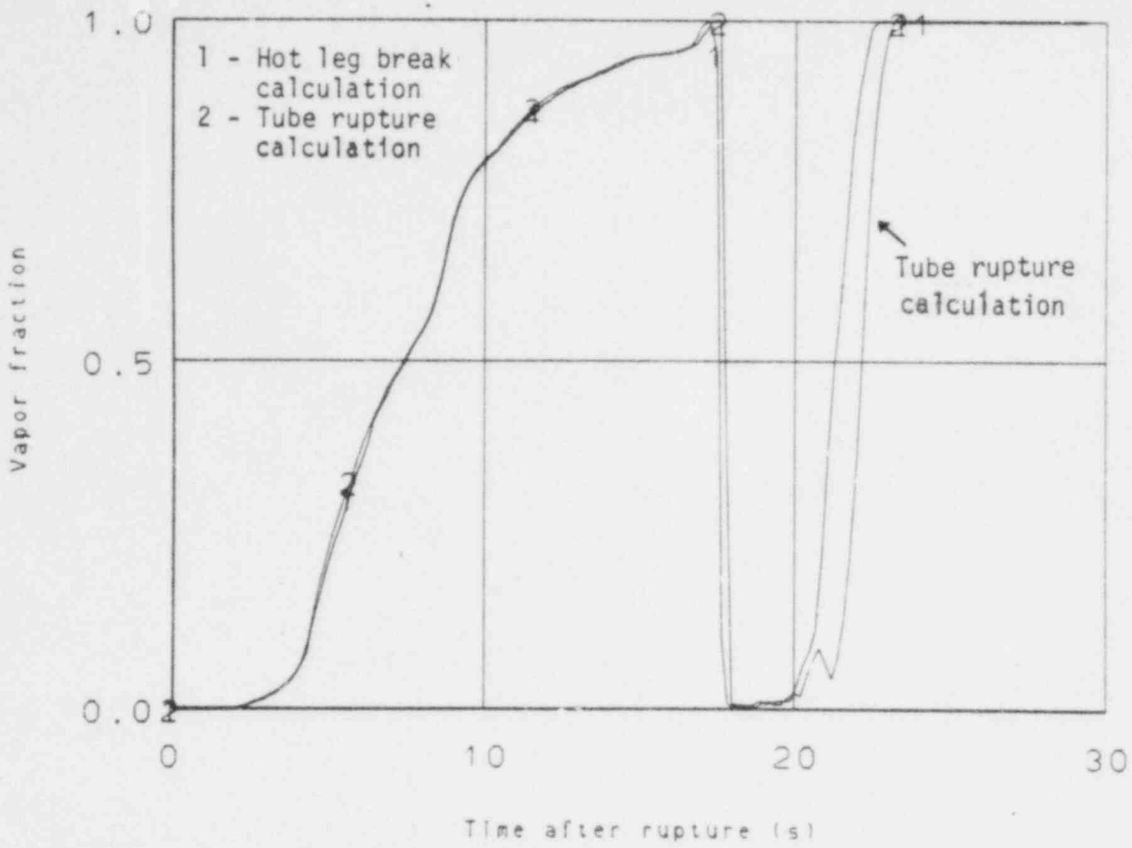

Figure 30. Intact loop (Loop 2) cold leg vapor fraction.

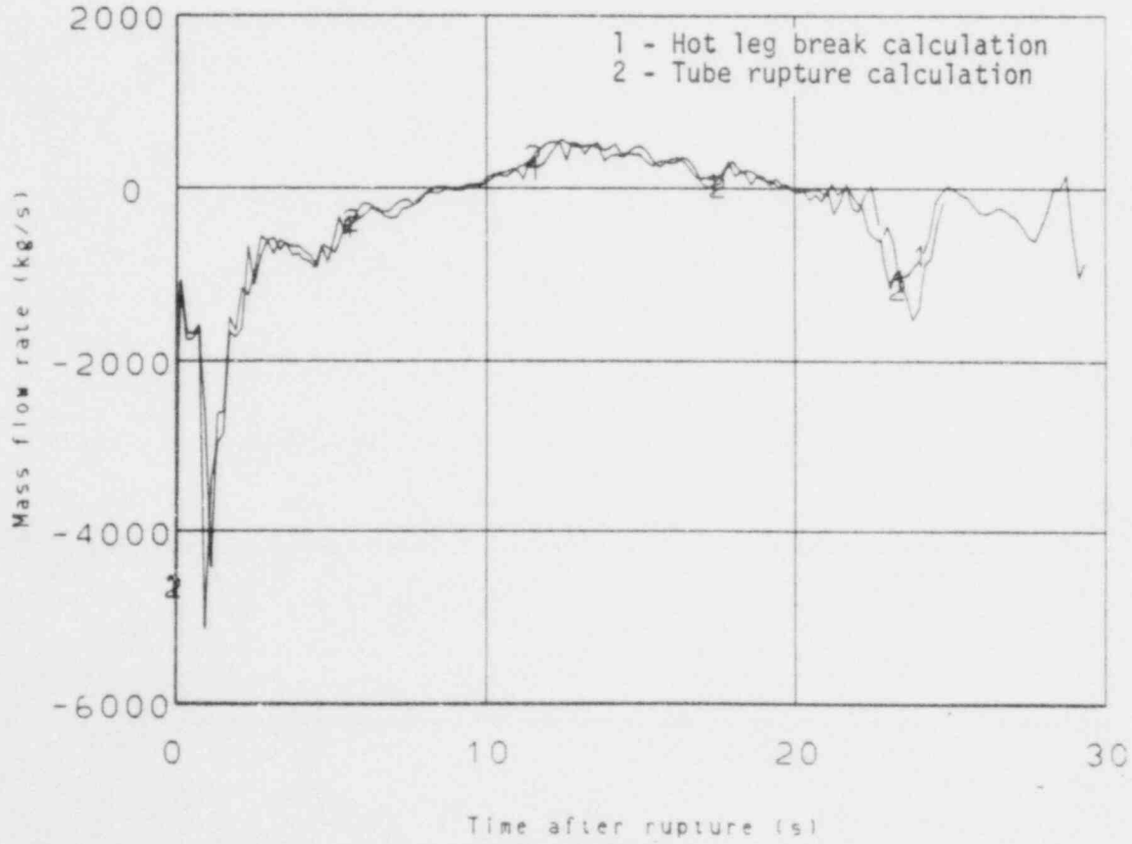

Figure 31. Intact loop (Loop 3) hot leg mass flow rate.

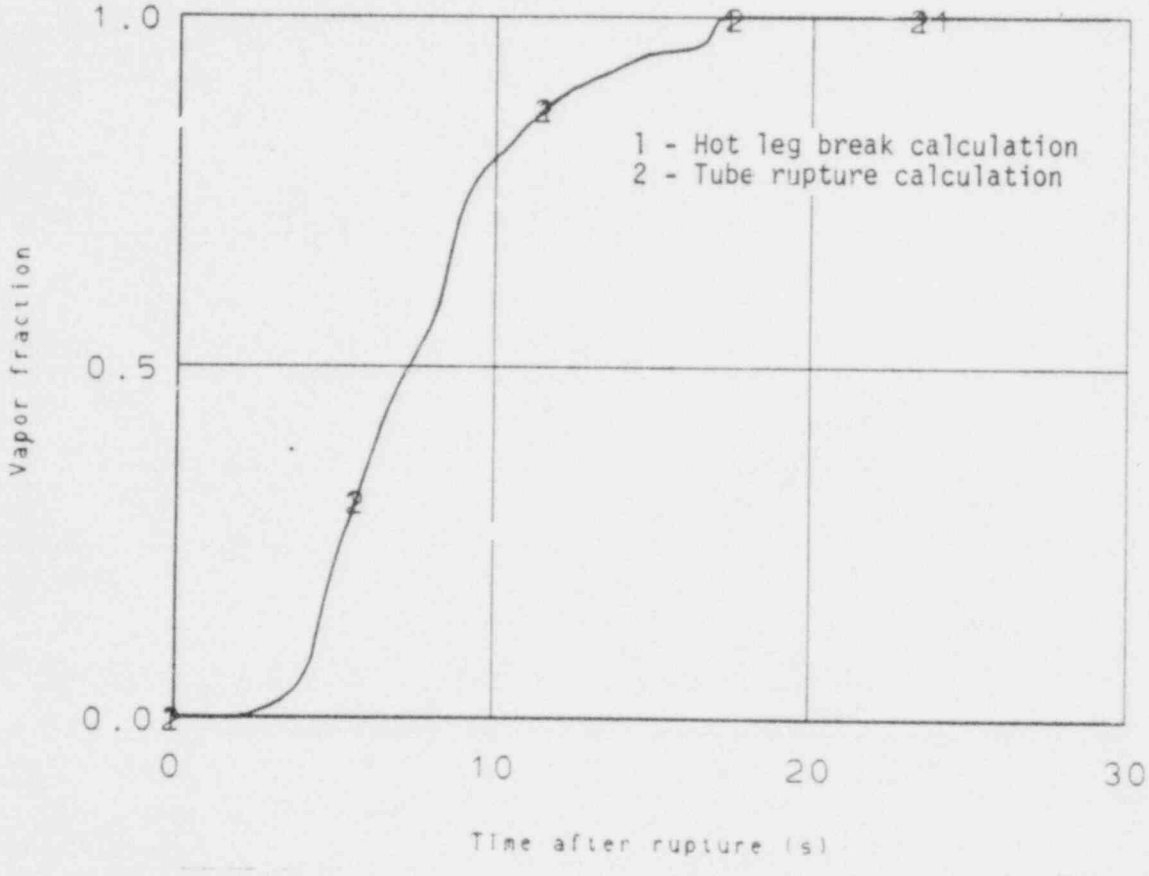

Figure 32. Intact loop (Loop 4) cold leg vapor fraction.

Figure 33. The void fraction remained high longer because of the delayed reflood as shown in Figure 34. The liquid level in the downcomer increased following accumulator and HPIS/LPIS injection. Because of the decreased core flow, the head in the downcomer was greater in the steam generator tube rupture calculation than in the hot leg break calculation. The larger head in the downcomer allowed the core to reflood at a faster rate as shown in Figure 34. The rods had completely quenched by 23.2 s in the tube rupture calculation, whereas in the hot leg break calculation the rods had quenched by 22.0 s.

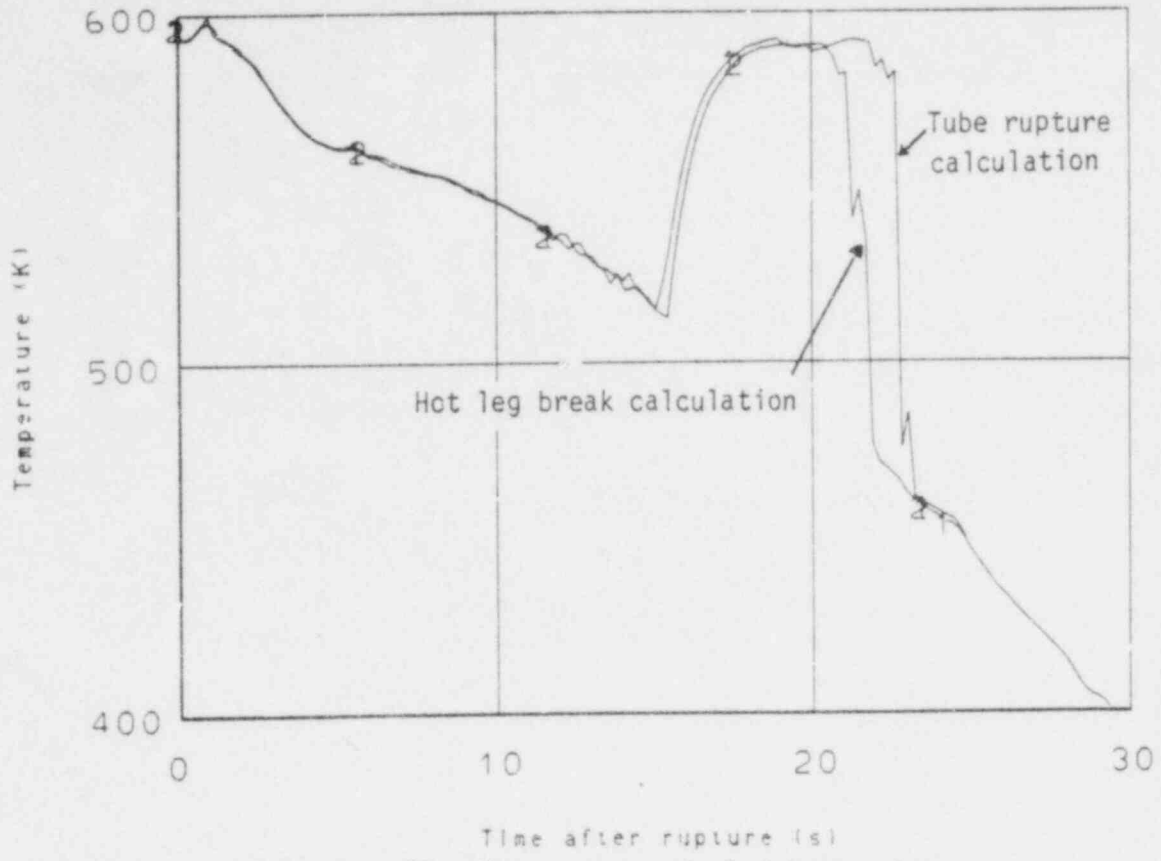

Figure 33. Upper core rod clad temperature.

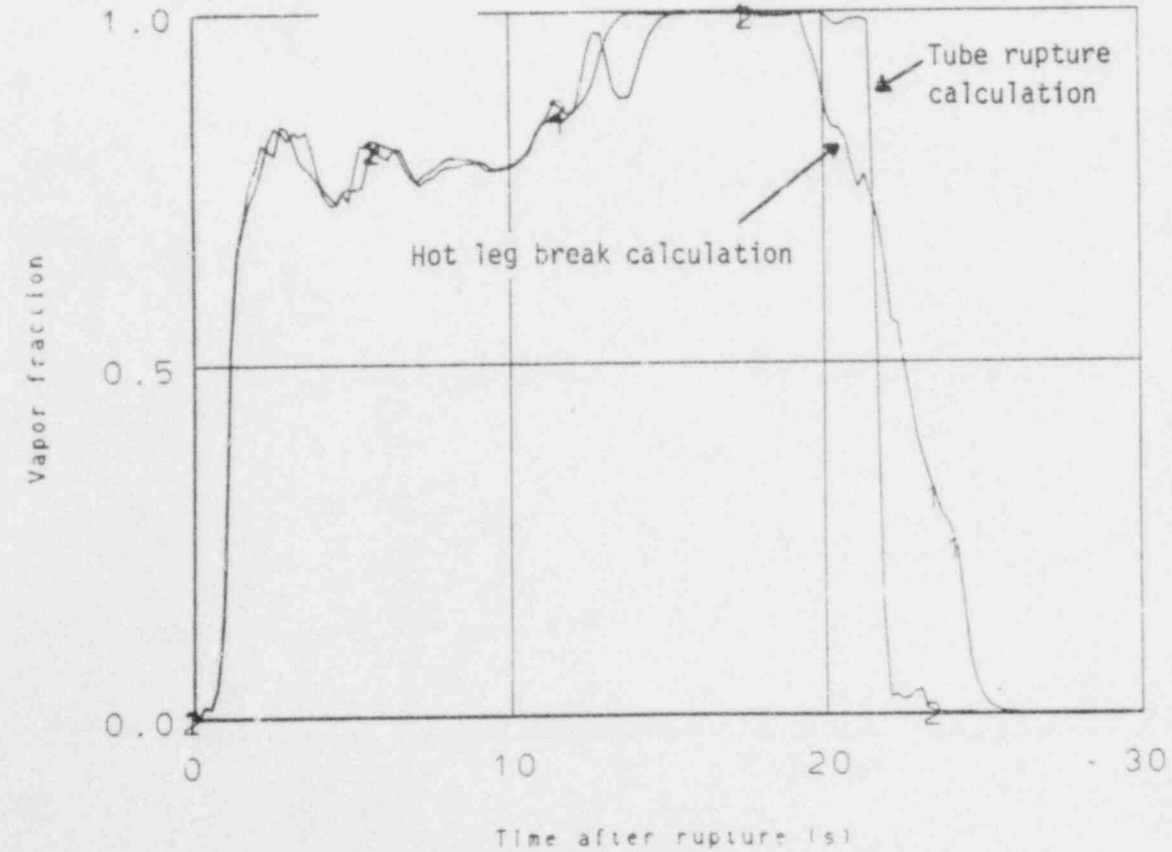

Figure 34. Vessel core void fraction (Level 8; Cell 5).

4. CONCLUSIONS

1. *The TRAC-P1A computer code adequately calculated the thermal-hydraulic behavior of the hot leg break transients.*

   Core mass flow remained positive throughout the calculations. Flow patterns within the vessel, during the calculations, looked reasonable. Lower plenum refill and core reflood occurred within a reasonable time. Rod clad temperature behavior was adequate. The calculations satisfactorily predicted the system behavior when compared to Semiscale test data.

2. *The effects from ruptured tubes in a steam generator was adequately predicted by the TRAC-P1A computer code.*

   Steam binding effects from the tube rupture prolonged core reflood and rod clad temperature quench time.

3. *Further investigation into vessel modeling should be performed.*

   The unexplained high vapor fractions in the azimuthal sections connected to the break should be investigated further. Different vessel modeling techniques may allow the vessel response to behave more reasonably.

5. REFERENCES

1. J. R. Larson, Calculations of a Large Cold Leg Break with Steam Generator Tube Ruptures in a PWR Using the TRAC-P1A Computer Program, EG&G Idaho, Inc., EGG-CAAP-5183, June 1980.

2. P. D. Wheatley, TRAC-P1A Calculations for a 200%, 0.25 m Diameter and 0.10 m Diameter Cold Leg Break in a Pressurized Water Reactor, EG&G Idaho, Inc., EGG-CAAP-5190, June 1980.

3. G. W. Johnsen, et al., A Comparison of "Best Estimate" and "Evaluation Model" LOCA Calculations; The BE/EM study, EG&G Idaho, Inc. PG-R-76-009, December 1976.

4. TRAC-P1A, An Advanced Best-Estimate Computer Program for PWR LOCA Analysis, LA-7777-MS, May 1979.

5. Zion Station Final Safety Analysis Report, Docket No. 50-295 (with amendments).

6. J. Sicilian, "TRAC Newsletter, Number 1", Los Alamos Scientific Laboratory, July 1979.

7. J. C. Vigil et al., TRAC-P1A Developmental Assessment, LA-8056-MS, October 1979.

8. H. S. Crapo et al., Experimental Data Report for Semiscale Mod-1 Test S-02-1 (Blowdown Heat Transfer Test), Aerojet Nuclear Company, INEL, UC-78a, July 1975.

ATTACHMENT NOT FILMED

ANO. 8007280178

NO. OF PAGES 2 microfiche

☐ DUPLICATE: ALREADY ENTERED INTO SYSTEM
UNDER ANO. _____

☐ ILLEGIBLE: HARD COPY AT:
- ☐ PDR
- ☐ CF
- ☑ OTHER ~~Microfiche~~ Cards

APPENDIX A

CODE INPUT LISTING

The following describes the input to the TRAC-P1A code to model the 200% hot leg break and the 200% hot leg break simultaneous with a rupture of 16 steam generator tubes.

TRAC-PIA input for 200% hot leg break.

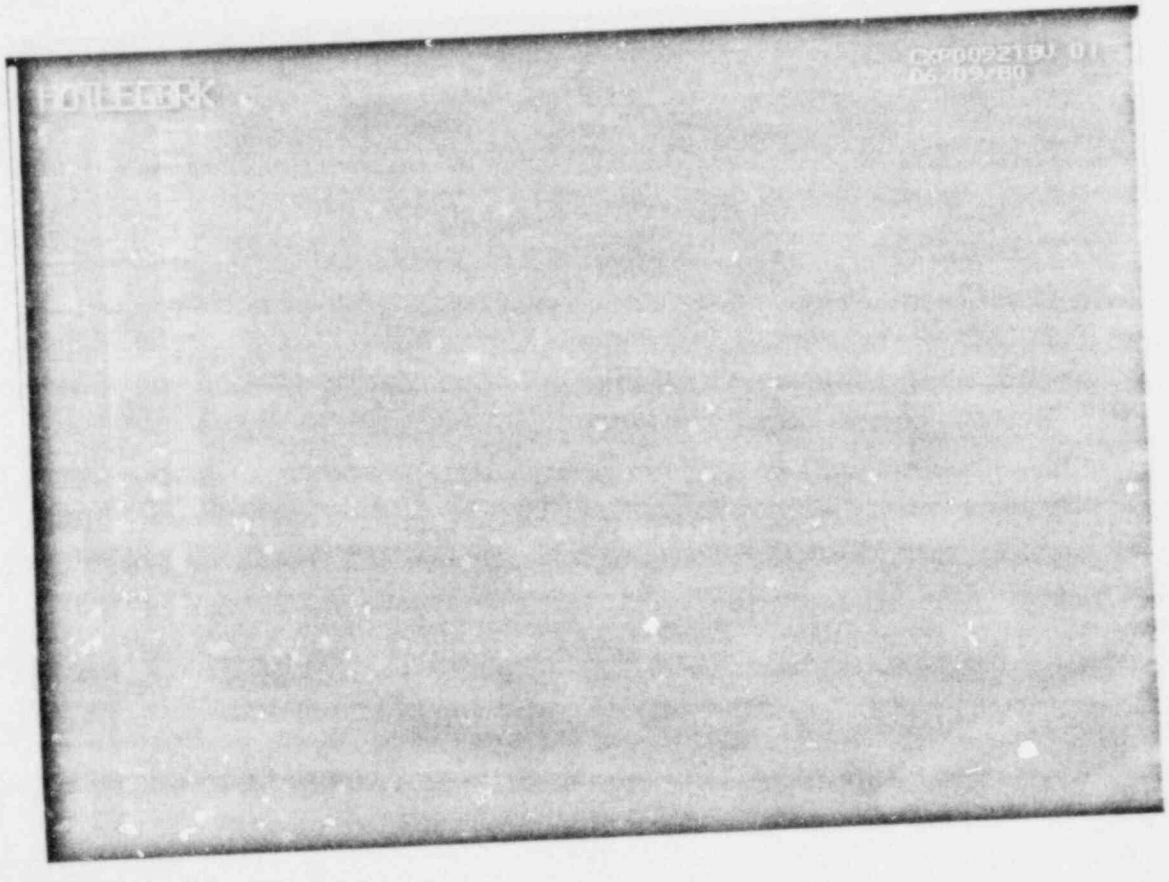

TRAC-PIA input for 200% hot leg break simultaneous with a rupture of 16 steam generator tubes.

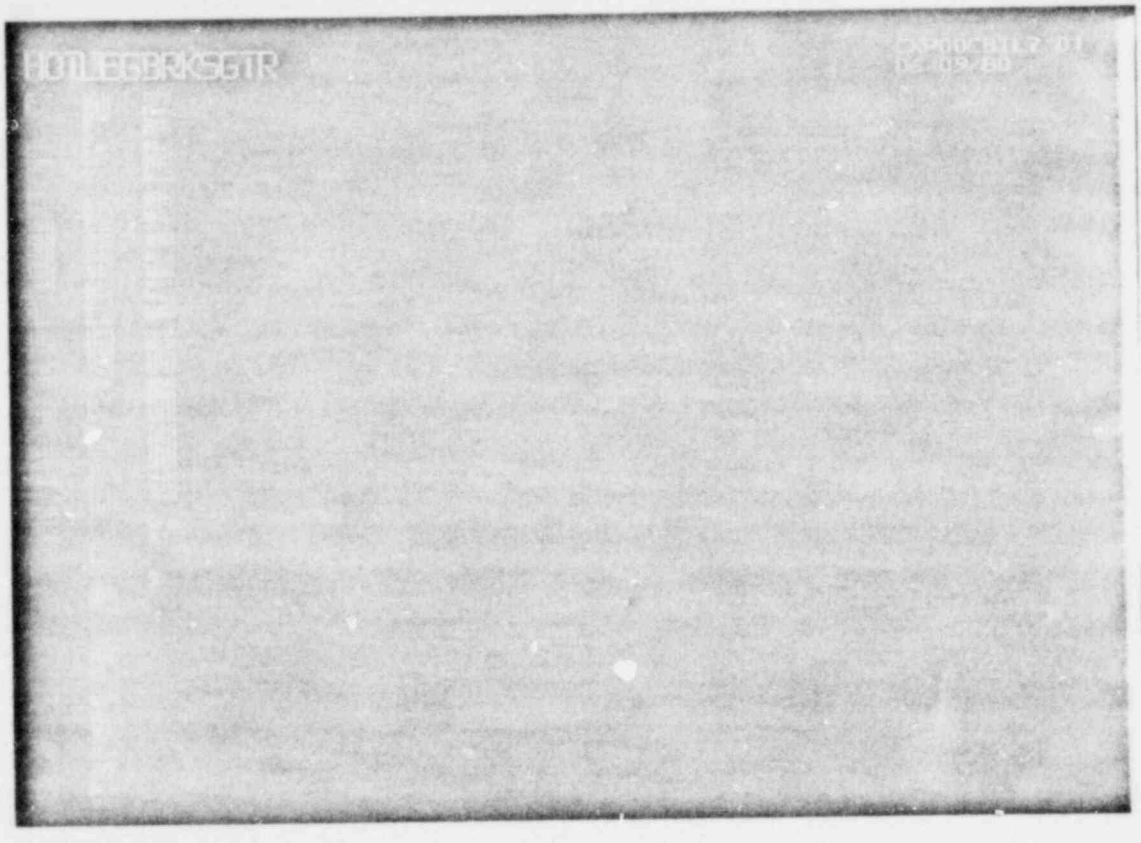

APPENDIX B

NODALIZATION OF MODEL COMPONENTS

The following describes the nodalization of the vessel, pressurizer, accumulators, breaks, ECC injection and steam generator tube rupture.

1. VESSEL

The axial and radial noding of the vessel is shown in Figure B-1. The nodalization consisted of 12 axial levels with each level subdivided into 3 radial and 8 azimuthal zones for a total of 288 mesh cells. The noding is somewhat different than used in the BE/EM[B-1] or USPWR1[B-2] models. Table B-1 shows the vessel fluid volumes, heat slab areas, and heat slab masses used in these calculations.

The downcomer region was modeled by the outer ring between levels 3 and 10. The downcomer lumped two actual flow paths on each side of the thermal shield. The barrel-baffle region which provides an additional flow path parallel to the downcomer was not included explicitely in the model. Its volume, surface area and mass were evaluated in the outer core ring. The flow path was not included.

The lower plenum was noded by three levels. The portion below the downcomer was divided into 2 levels to permit backflow from the core to the downcomer without removing residual liquid from the bottom of the vessel. Level 3 of the lower plenum lies at the bottom of the active core and includes structures such as the core support plate and core mixing plate.

The core consists of 5 axial levels and 2 radial rings. The top of vessel level 8 corresponds to the top of the active fuel. This noding provided a means for representative axial and radial power distribution in the core.

The fuel rod was divided into 9 cells for the fuel, one cell for the pellet-cladding gap and one cell for the cladding. A radial power distribution was input to the fuel pellets and is described in a following section.

The upper plenum was noded by three levels, level 9 below the inlet and outlet nozzles, level 10 which was sized to span the outlet nozzle flow

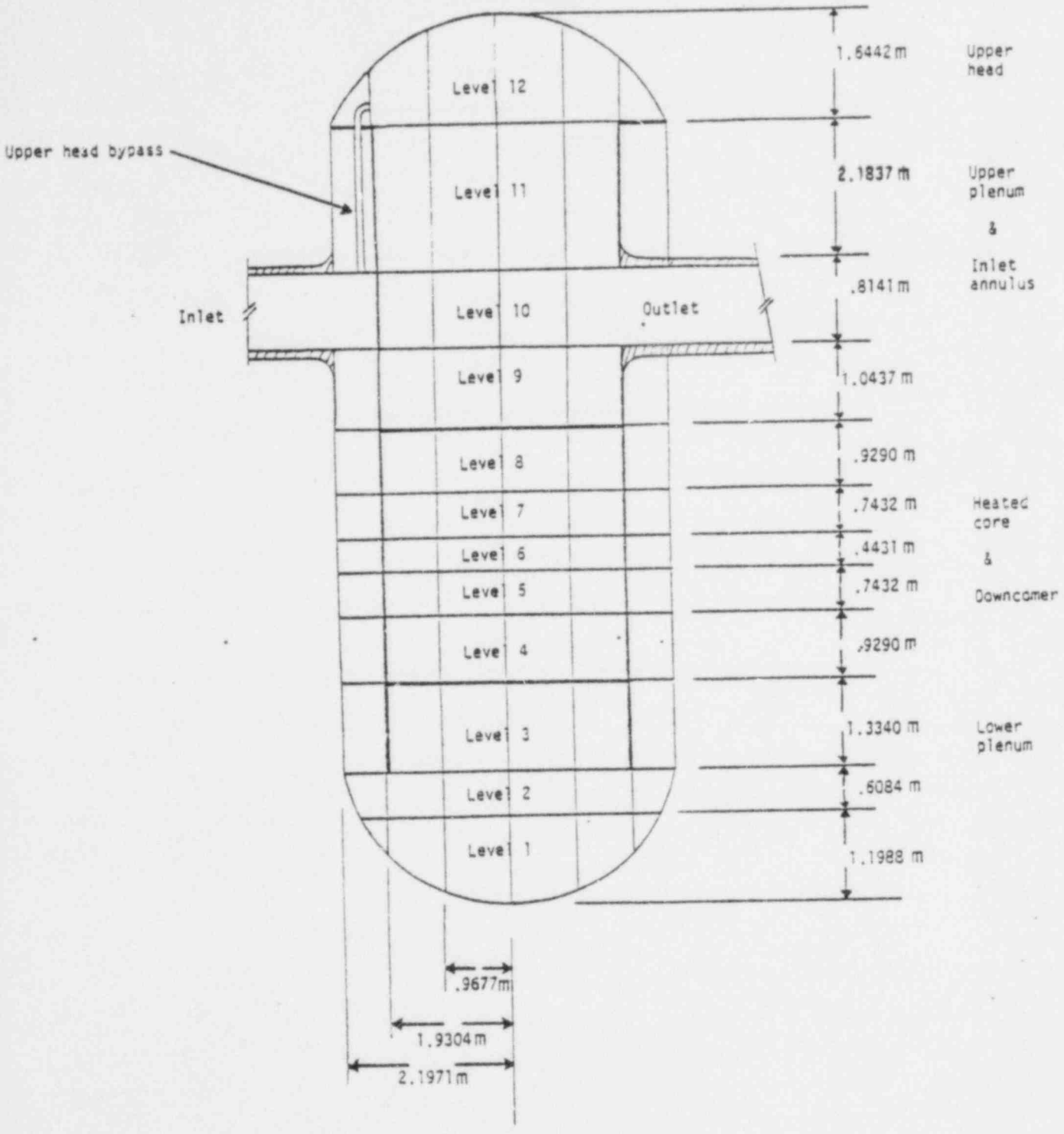

Figure B-1. Vessel noding for TRAC.

TABLE B-1. COMPARISON OF VESSEL VOLUMES, HEAT SLAB AREAS AND HEAT SLAB MASSES

Lower Plenum Heat Slab Area (m^2)	Lower Plenum Heat Slab Mass (kg)	Lower Plenum Liquid Volume (m^3)	Downcomer Liquid Volume, Core Section (m^3)	Core Liquid Volume (m^3)	Downcomer Heat Slab Area, Core Section (m^2)
180.32	29160.0	28.57	9.68	18.32	195.79

Core Heat Slab Area (m^2)	Core Heat Slab Mass (kg)	Upper Plenum Volume (m^3)	Upper Plenum Heat Slab Area (m^3)	Inlet Annulus Volume (m^3)	Upper Head Volume (m^3)	Loop Flow Volume (m^3)
717.73	10306.0	40.31	329.62	9.31	13.67	42.69

area, and level 11 above the nozzles and below the upper head. Level 12 represented the upper head region of the vessel.

2. PRESSURIZER AND ACCUMULATORS

Figure B-2 shows the cell nodalization used for the pressurizer. The accumulators were nodalized in a similar manner. This type of model was recommended for the pressurizer at the TRAC Workshop[B-3] held at LASL in February, 1980.

Basically, the bottom of the pressurizer and accumulators was modeled by a very short node. The connecting cell of the joining tee was also noded the same length as the adjoining pressurizer or accumulator cell but with a flow area equal to that of the pressurizer or accumulator. The appropriate initial liquid volume was obtained by including the connecting tee cell volume as part of the desired pressurizer or accumulator component volume. The fully implicit hydrodynamics option differencing technique was used on the secondary side of the tee to avoid Courant limiting of the time step size and to provide a better representation of the pressure drop calculated at the junction of the components. Using the semi-implicit hydrodynamics option too high a pressure drop and a smaller mass flow rate would be calculated at the junction if the tee cell was small in diameter compared to the pressurizer cell. Table B-2 shows the pressurizer and accumulator volumes.

3. BREAKS

The break piping was nodalized following the guidelines presented in the TRAC-P1A Developmental Assessment Report.[B-4] The nodalization is shown in Figure B-3 for the hot leg and cold sides (PIPE 1 and PIPE 75). The hot leg break location was located just outside the biological shield.

A short test run was made with a coarser spacing but little change was noted. Thus it was felt that the selected nodalization was adequate.

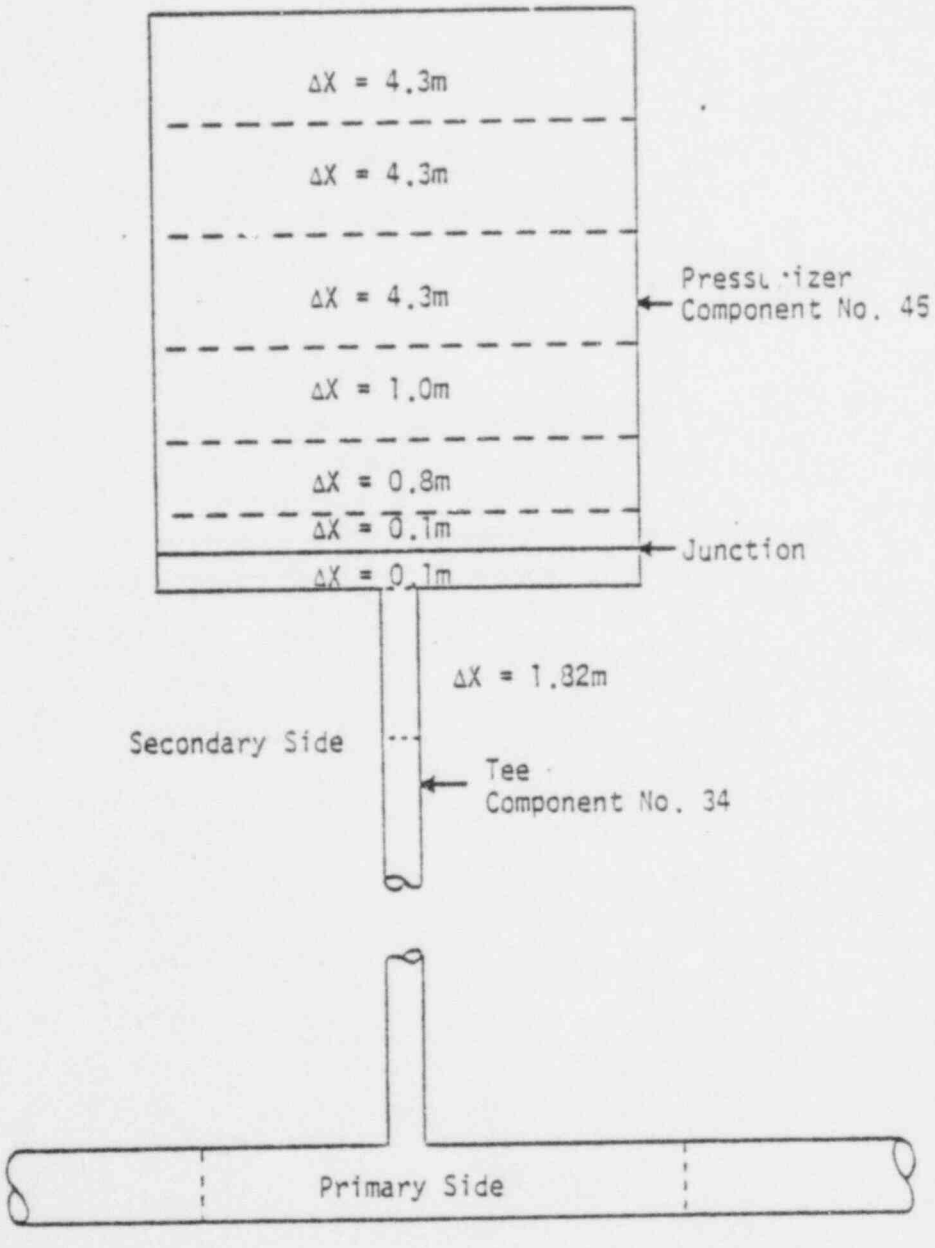

Figure B-2. Nodalization of pressurizer and connecting Tee showing all cell lengths.

TABLE B-2. PRESSURIZER AND ACCUMULATOR VOLUMES

Pressurizer Volume (m^3)	Accumulator Volume (m^3)
30.32	26.88

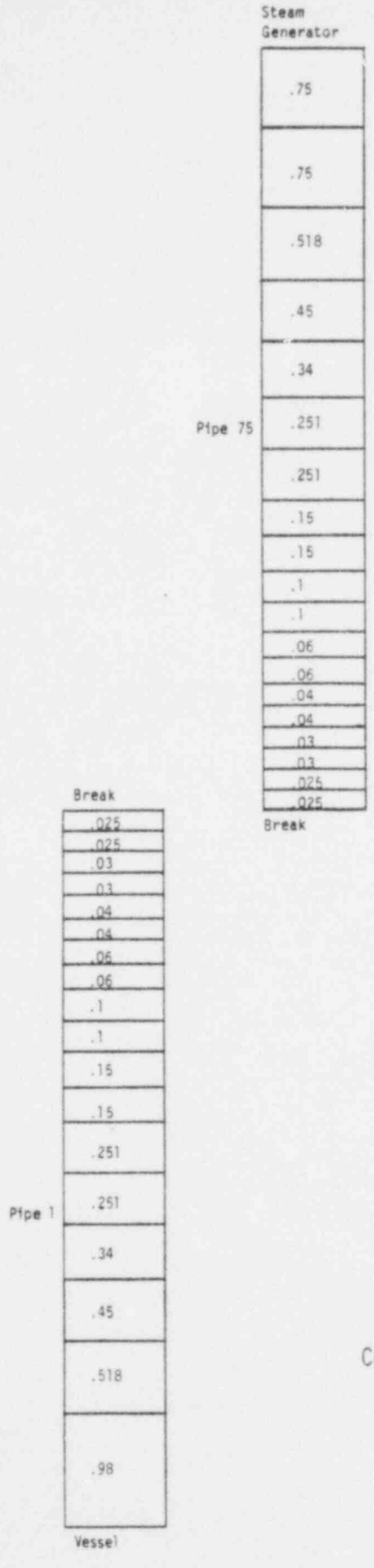

Cell lengths in meters.

Figure B-3. Break nodalization for 200% hot leg break calculations.

4. ECC INJECTION

The fill components for each loop lumped together the charging and safety injection systems. The mass flow rates were specified to be equal for each loop and were a function of the local pressure. The mass flow rate as a function of pressure was taken from the BE/EM study for the intact loop and converted to velocity for input to the TRAC code.

5. STEAM GENERATOR RUPTURE

The TRAC computer code steam generator component model does not permit direct simulation of a tube rupture permitting flow communication between the primary and secondary sides. Thus, to simulate ruptured tubes at the tube sheet on the inlet side of the steam generator a VALVE component 18 was connected to TEE 12 as shown in Figure B-4. The component model of the steam generator and valve was used to investigate potential problems with the configuration and size the valve opening to obtain the appropriate mass flow rate. The component consisted of a converging-diverging nozzle with a valve to provide a means of adjusting the flow area.

The appropriate mass flow rate was obtained from Semiscale test results[B-5] which showed a maximum peak cladding temperature for a particular mass flow rate from a simulated rupture in the steam generator. The mass flow rate for the PWR was determined by applying core area scaling to the Semiscale results. Different scaling criteria would lead to different mass flow rates. The Semiscale tests were run from conditions simulating the steam generator and primary system after blowdown. Therefore, the valve area was sized with the primary side of the steam generator and piping kept at 0.25 MPa. The secondary side was initialized at conditions corresponding to steady state operation.

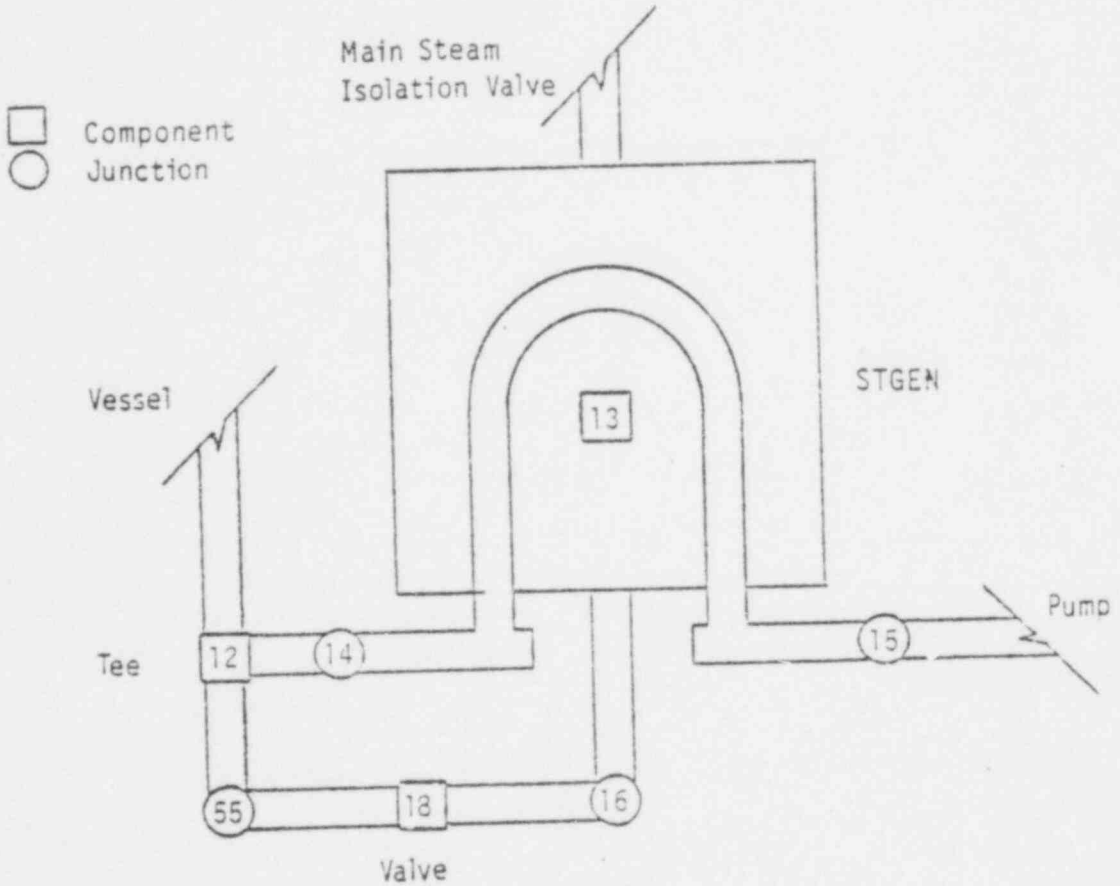

Figure B-4. Steam generator tube rupture model for the 200% hot leg break simultaneous with a rupture of sixteen steam generator tubes.

The desired mass flow rate was determined in the following manner for the rupture. The mass flow rate from 16 ruptured tubes as determined in the reference was scaled by the ratio of the Semiscale and PWR core flow areas, ie,

$$\frac{\text{leakage mass flow rate (PWR)}}{\text{core flow area (PWR)}} = \frac{\text{leakage mass flow rate (SS)}}{\text{core flow area (SS)}}$$

Substituting in this ratio and solving for the PWR leakage mass flow rate yielded,

$$9.07^{-3}\ \frac{\text{Kg}}{\text{s}}\ \begin{matrix}\text{scaled}\\ \text{per tube x 16 tubes}\\ \text{for SS}\end{matrix} \times \frac{4.933\ \text{m}^2\ \text{(Zion I core flow area)}}{4.768 \times 10^{-3}\ \text{m}^2\ \text{(Semiscale core flow area)}}$$

$$= 150.1\ \frac{\text{Kg}}{\text{s}}$$

Figure B-5 shows the geometry of the symmetric nozzle for the small rupture.

To obtain the correct heat transfer from the primary side to the secondary side of the steam generator it was necessary to lower the back pressure at the secondary side break from 5.24 to 4.6 MPa. Also to obtain a steady state mass balance across the secondary side it was necessary to increase the main feedwater mass flow to about 800 kg/s from the specified 440.7 kg/s.

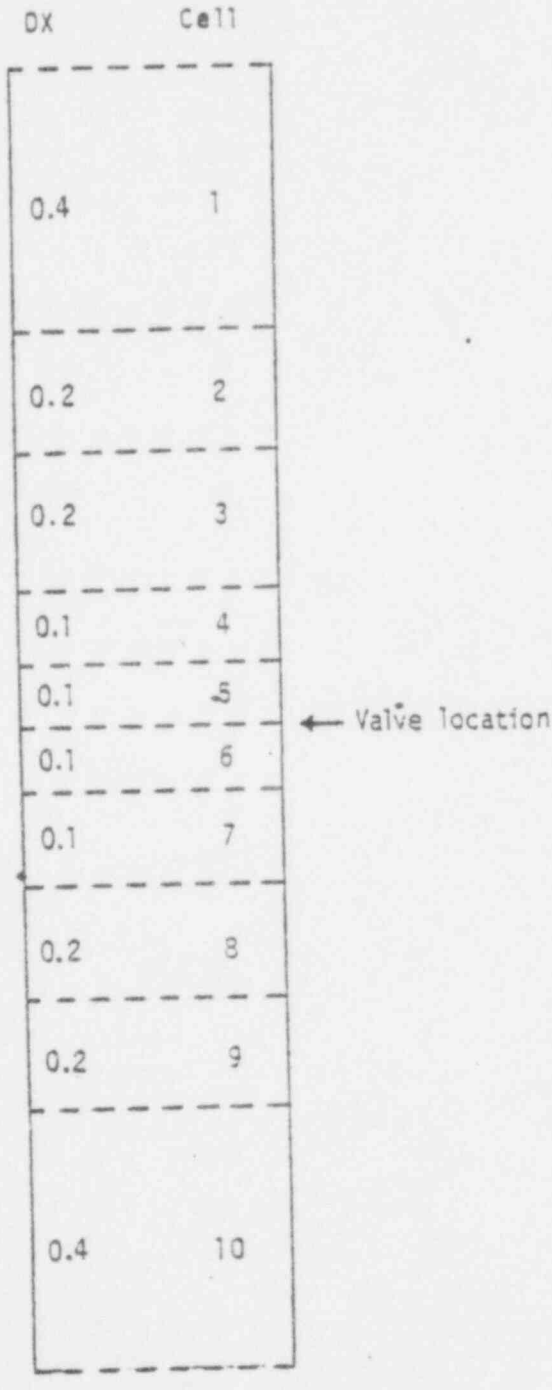

Figure B-5. Nodalization of valve simulating 16 ruptured steam generator tubes.

REFERENCES

B-1. G. W. Johnsen et al., A Comparison of "Best Estimate" and "Evaluation Model" LOCA Calculations: The BE/EM Study, EG&G Idaho, Inc., Report PG-R-76-009, December 1976.

B-2. TRAC-P1A, An Advanced Best Estimate Computer Program for PWR LOCA Analysis, LA-7777-MS, May 1979.

B-3. J. K. Meier, "Problem Modeling", TRAC Workshop, Los Alamos, New Mexico, February 6, 1980.

B-4. J. C. Vigil et al., TRAC-P1A Developmental Assessment, LA-8056-MS October 1979.

B-5. J. M. Cozzuol, O. M. Hanner, G. G. Loomis, Investigation of the Influence of Simulated Steam Generator Tube Ruptures During Loss-of-Coolant Experiments in the Semiscale Mod-1 System, TREE-NUREG-1213, May 1978.

APPENDIX C

COMPONENT INITIAL AND BOUNDARY CONDITIONS

This section describes the initial and boundary conditions of the model components.

1. CORE POWER DISTRIBUTION

The relative axial power distribution for the 5 core levels is shown in Table C-1. The distribution is very similar to the BE/EM study.[C-1] Slight differences occurred because the BE/EM study included vessel structure and volume above and below the active core in the top and bottom core volumes and the core was divided into 6 core levels.

The relative core radial distribution is shown in Table C-2. The distribution was obtained from a report on Zion I fuel performance[C-2] by averaging the peaking factors given for each fuel assembly within the inner and outer rings of the model corresponding to the core. The axial and radial distributions resulted in an average rod peak steady state power density of 31.73 Kw/m (9.67 Kw/ft). The decay heat generation was based on the ANS specification and was taken from the BE/EM study.

The relative fuel rod radial power distribution is shown in Table C-3. The distribution was obtained from Reference C-2.

2. PUMPS

The primary loop circulating pumps were left on throughout the transient calculation.

3. SAFETY INJECTION FLOW

The safety injection and charging systems were combined into one fill for each loop. The mass flow injected as a function of local pressure is shown in Figure C-1.

4. STEAM GENERATORS

Steam flow from the secondary side of the steam generators was shut off by linearly closing the valve upstream of the break between 0.0 s and 1.5 s. The feedwater was terminated and auxiliary feed was begun

TABLE C-1. RELATIVE CORE AXIAL POWER DISTRIBUTION

Core Level	Factor
1 bottom	0.8142
2	1.189
3	1.20
4	1.1706
5 top	0.7018

TABLE C-2. RELATIVE CORE RADIAL POWER DISTRIBUTION

Ring	Factor
1 inner	1.0898
2 outer	0.83373

TABLE C-3. RELATIVE FUEL ROD RADIAL POWER DISTRIBUTION

Node	Factor
1 centerline	0.967
2	0.969
3	0.972
4	0.977
5	0.984
6	0.992
7	1.003
8	1.016
9	1.037

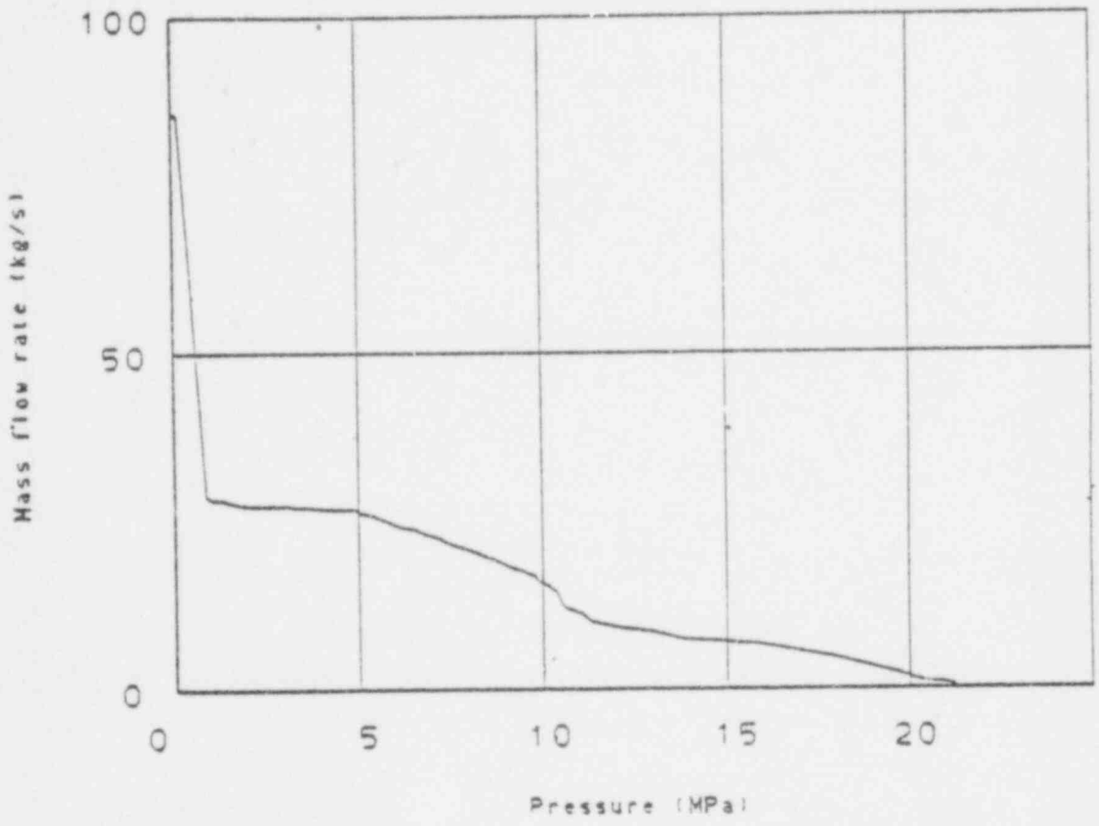

Figure C-1. ECC injection mass flow rate.

as shown in Figure C-2. The initial conditions for the secondary side of the steam generators are listed in Table C-4. The initial void fraction distribution and mass inventory could not be adjusted to obtain desired distribution or inventory.

5. SCRAM

Scram occurred at 0.53 s.

6. CONTAINMENT PRESSURE

The containment pressure is shown as a function of time in Figure C-3.

7. ACCUMULATORS AND PRESSURIZER

The initial conditions for the accumulators and pressurizer are listed in Table C-5.

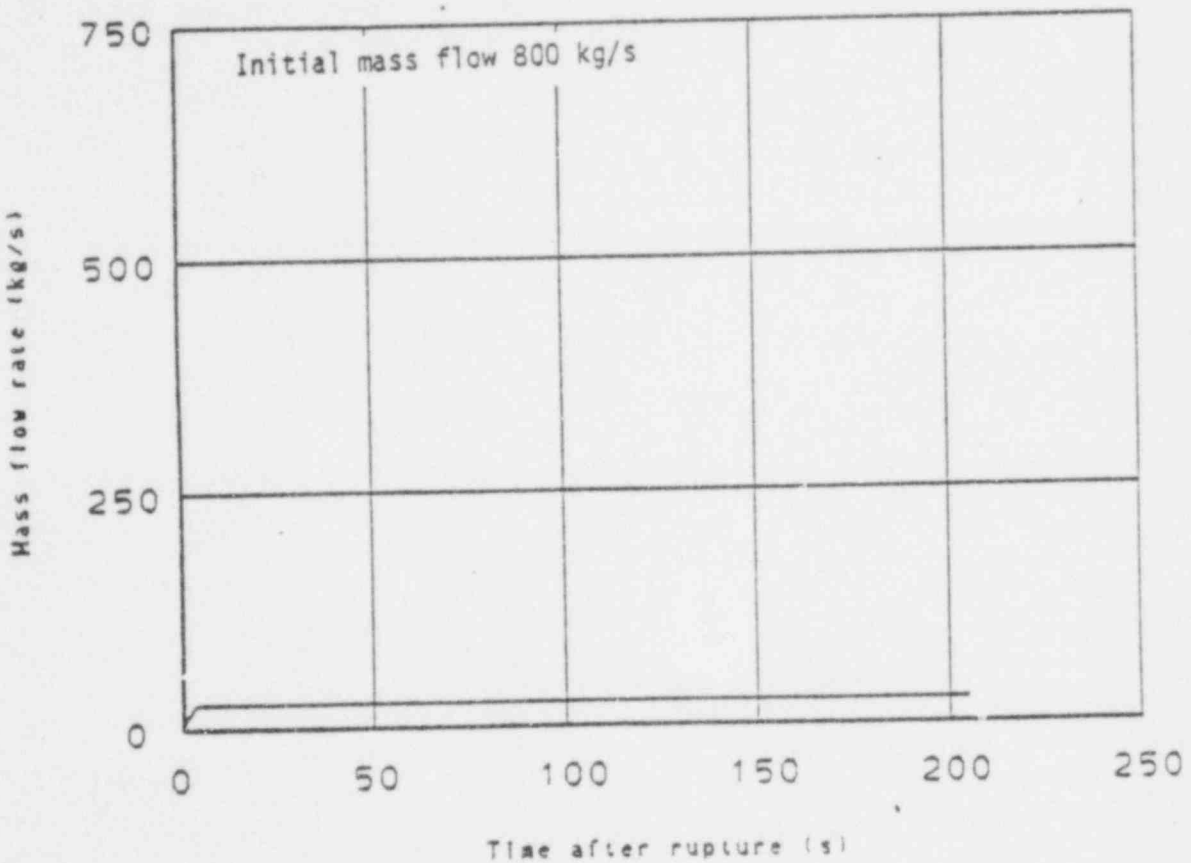

Figure C-2. Steam generator feedwater and auxiliary feedwater mass flow.

TABLE C-4. INITIAL CONDITIONS FOR MODELED STEAM GENERATOR SECONDARY SIDE COMPARED TO THE BE/EM STUDY

	MODEL	BE/EM
Backpressure (MPa)	4.6	5.25
Inlet Temperature (K)	493.0	493.0
Mass (kg)	51,500.0	40,000.0

TABLE C-5. INITIAL CONDITIONS FOR ACCUMULATORS AND PRESSURIZER

	Accumulators	Pressurizer
Pressure (MPa)	4.43	15.43
Temperature (K)	325.0	598.0
Trip Pressure (MPa)	4.08	

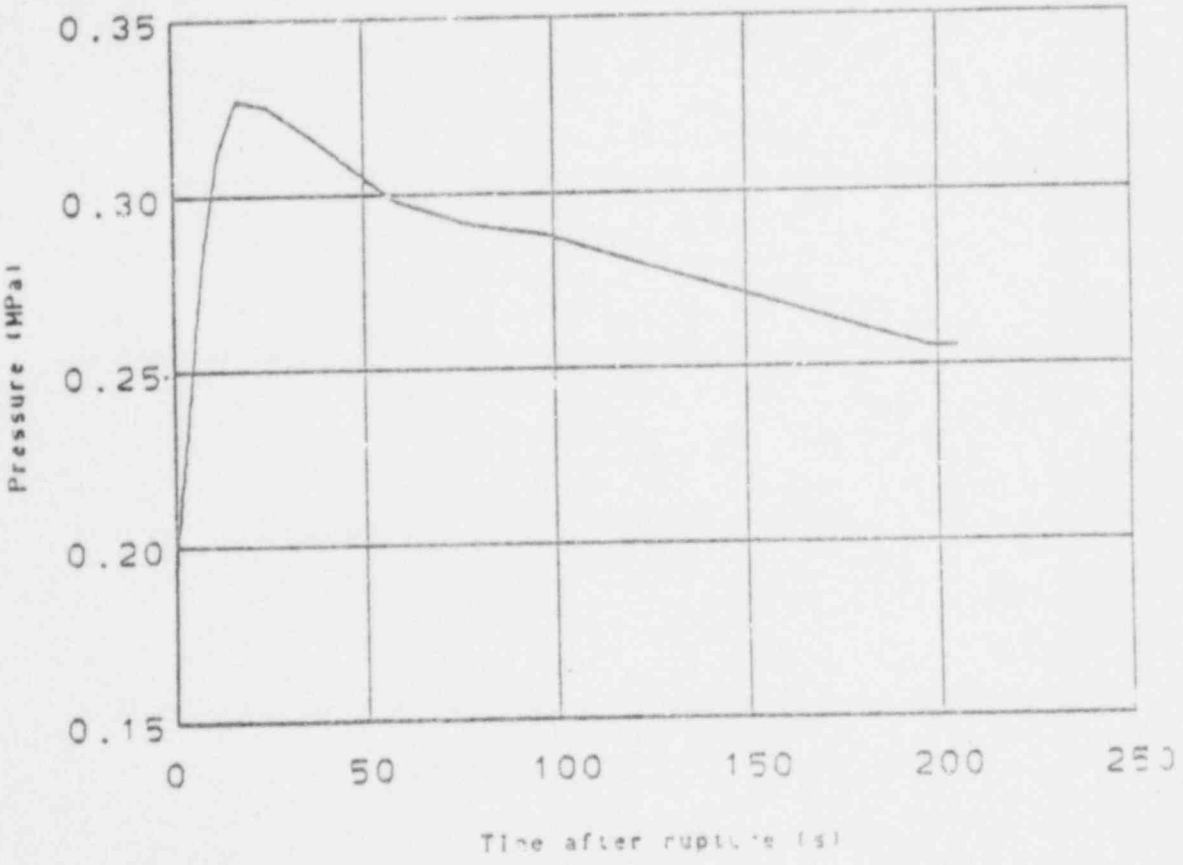

Figure C-3. Containment pressure.

REFERENCES

C-1. G. W. Johnsen et al., A Comparison of "Best Estimate" and "Evaluation Model" LOCA Calculations, The BE/EM study, EG&G Idaho, Inc., Report PG-R-76-009, December 1976.

C-2. H. H. Crain et al., Interim Report, Zion Unit 1, Cycle 1 Fuel Performance, Westinghouse Electric Corporation, WCAP-8837 December 1976.